Microfabrication Using Bulk Wet Etching with TMAH

Duan, Xuefeng

Master of Science

Department of Physics

McGill University

3600 University
Montreal,Quebec H3A 2T8

2005-8-31

A thesis submitted to McGill University
in the requirements of Master Degree in Science

Your file Votre référence
ISBN: 978-0-494-24657-3
Our file Notre référence
ISBN: 978-0-494-24657-3

ACKNOWLEDGEMENTS

The work presented in this thesis would not have been possible without the assistance of many people. Most of all, I thank Dr. Peter Grütter, my supervisor, for giving me the chance to work on the very promising and interesting field. He gives us the freedom to work on our own interests and always encourages us about our research progress.

Vito Logiudice, the fab manager, is always supportive and helpful. He spent a lot of time on discussing with me about my processes. His experience helped me a lot and his kindness made him a very easy-going man to get along with.

The technologists, Neal Lemaire and Don Berry, deserve many thanks for getting me familiar with the equipment in the fab. Here, I thank them for those early mornings and late evenings that they stayed with me.

I would also thank Matthieu Nannini. He did a lot of tests in the fab, and set up a lot of recipes in the yellow room. In addition, I would like to thank Shawn Foster, a member in our group. He communicated with me a lot about the experience of microfabrication.

Lastly, I would thank my friends outside my work. They make me not feel alone in Canada.

ABSTRACT

In November 2002 a Microfabrication Lab was established in the physics department of McGill University to support research in nanoscience and technology. At the same time, I arrived at McGill to begin my graduate study. So I was assigned to do research on microfabrication, especially bulk wet etching of silicon using TetraMethyl Ammonium Hydroxide (TMAH).

The content of microfabrication is quite broad, and also very useful in both industry and academic. Since our fab is a newly built one and I had no experience in this area before, this thesis mainly included some basic processes in microfabrication, such as the photolithography, wet etching, reactive ion etching, and so on. Also it compared the wet etching with dry etching. Some results of TMAH wet etching were showed in the thesis, which agreed well with that of the other groups. A simulation program was developed to predict the etching result of TMAH and it appeared to work well. Finally, based on the knowledge and experience acquired, processes in making cantilever and tip structures, which are critical in the scanning probe microscopes, were developed. Silicon oxide cantilevers with length of 100-200 μm, width of 30-50 μm, and thickness of 1 μm were obtained. Pyramid like silicon tips were also fabricated using the wet etching.

ABRÉGÉ

En Novembre 2002, un centre de micro et nanofabrication a été inauguré au sein du département de physique de l'université McGill afin d'apporter un support à la recherche en nanoscience et nanotechnologie. C'est à ce moment que je suis arrivé à McGill pour commencer ma maîtrise. Mon projet fût ainsi directement relié à ce nouveau laboratoire à travers l'étude de la gravure humide de silicium dans une solution de TetraMethyl Ammonium Hydroxide (TMAH).

Étant donné que la salle blanche vient juste de voir le jour et que je n'ai aucune expérience dans ce domaine, une large partie de mon travail consistait à me rendre plus familier aux principes de la gravure humide ainsi qu'aux méthodes de microfabrication disponibles en la salle blanche. Ce mémoire décrit un important procédé de base : la gravure humide du silicium.

Le premier chapitre introduit le lecteur à certains concepts et applications des techniques de microfabrication. Deux techniques majeures sont comparées : gravure humide et gravure sèche. Le chapitre deux se concentre sur les profils de gravure produits avec le TMAH ce qui est un élément très important en microfabrication. De nombreux procédés et masques utilisés pour fabriquer des microstructures sont basés sur ce savoir faire. Le chapitre trois présente un problème qui nécessite une considération élevée quand on doit concevoir un procédé ou un masque. Les taux de gravures anisotropiques caractéristiques du TMAH conduisent, lors de la gravure, à une déformation des structures dessinées sur le masque. Ceci peut être compensé par un design de masque basé sur des simulations de la gravure anisotropique. Le

chapitre quatre présente quelques applications de base de la gravure anisotropique comme la réalisation de cantilever pour la microscopie à force atomique.

TABLE OF CONTENTS

LIST OF TABLES

LIST OF FIGURES

CHAPTER 1
Introduction to Microfabrication

1.1 Introduction

Science and technology have always pushed towards miniaturization. In the late 1980s, single atoms were manipulated by scanning tunnelling microscope [1]. The STM has a probe as sharp as an atom at the tip. When the distance between the tip and a flat specimen is approximately 1 nm and kept constant by monitoring the tunnelling current, it is possible to extract a single atom from the surface of the specimen by applying a voltage pulse and then place it at a desired position. Many experiments were then performed all over the world to write letters and draw figures by arranging atoms [2]. The same apparatus is also useful for observing molecular shapes, manipulating single molecules and modifying them.

In order to interface to the nano world, micron scale structures are necessary to bridge the gap to the macroscopic world. Methods of microfabrication, well established and developed for microelectronics applications such as the fabrication of integrated circuits, can be used to micromachine structures in 3D indispensable to interface to the nano world. Micromachining already has many industrial applications, such as the accelerometer that triggers air bags in cars [3] or mass storage devices [4]. Micromachining also has many applications in research and development. For example, the atomic force microscope(AFM) plays an important role in nanoscience research. The crucial component of the AFM is a micromahined cantilever with an integrated, sharp tip [5]. The purpose of my research is to understand the bulking wet micromachining, and to use this technique to fabricate SPM probes, such as cantilevers.

Microfabrication mainly uses the top-down approach, that means bulk materials or thin films are shaped into microstructures using lithography and etching or very precise cutting tools. It is often based on semiconductor processes, using silicon as a substrate. Table 1-1 gives some commonly used micromachinning processes [6].

Table 1–1: Partial List of Subtractive Processes Important in Micromachining

Subtractive Technique	Applications	Typical Etch Rate	Remark
Wet Chemical etching	cantilevers bridges, grooves	from $1\mu m/min$ to $50\mu m/min$	simple but poor control
Electrochemical etching	Etch stop technique	p-Si etching at 1.25-1.75$\mu m/min$	complex, require electrode
Dry chemical etching	Resist stripping Isotropic features	Typical Si etch rate $0.1\mu m/min$	Resolution better than $0.1\mu m$
Phys./Chem. etching	Very precise pattern transfer	Typical Si etch rate $0.1 - 1\mu m/min$	Most important of dry etching
Focused ion-beam milling	microsturctures in arbitrary materials	Typical Si etch rate $1\mu m/min$	Long fabrication time

So it is important to evaluate all the presented micromanufacturing methods before deciding on one specific machining method optimal for the application at hand.

1.2 Bulk Micromachining

In the early stage of microfabrication, many kinds of chemical solutions, including acid and base, were used to selectively remove significant amounts of silicon from a silicon wafer. In this case, micro structures could be formed by a chemical reaction of the silicon with the etchant. Below is a typical process for making a silicon nitride cantilever.

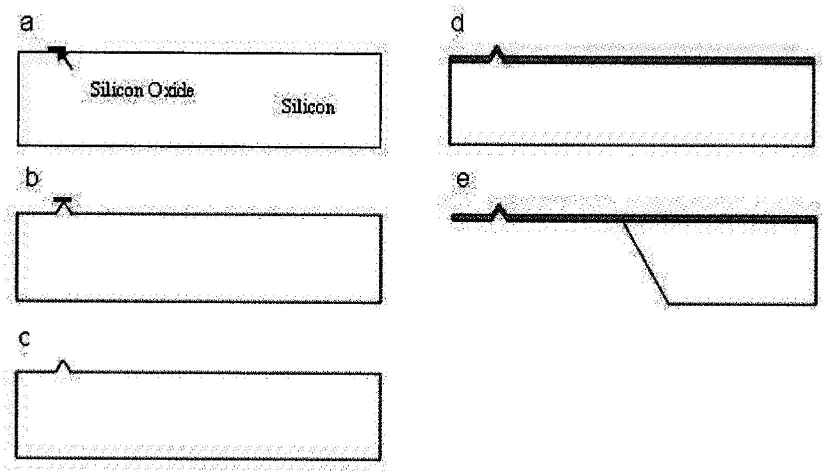

Figure 1–1: Process for making Silicon Nitride Cantilever. a)Pattern the front silicon oxide; b)TMAH wet etching to get the tip; c)Remove the silicon oxide; d)Silicon nitride deposition; e)Backside etching to release the nitride cantilevers

Despite the more recent emergence of higher resolution surface micromachining approaches, bulk micromachining is still widely in use. Particularly in light of newly introduced dry etching method ,such as plasma etching and reactive ion etching, bulk micromachining can now be used in combination with many other processes. So it is unlikely that bulk micromachining will decrease in popularity in the near future.

The available etching methods fall into two categories in terms of the state of the etchant: wet and dry.

1.2.1 Wet Etching

Isotropic Wet Etching

Isotropic etchants etch in all crystallographic directions at the same rate; they usually are acidic, such as "HNA", a mixture of hydrofluoric acid (HF), nitric acid (HNO_3), and acetic acid(CH_3COOH), and lead to rounded isotropic features in single crystalline silicon. The typical etch rate is several microns per minute. It is widely used for removal of work-damaged surfaces, rounding of sharp anisotropically etched corners to avoid stress concentration, removing of roughness and patterning.

Anisotropic Wet Etching

In anisotropic etching, the etch rate (ER) is much faster in certain direction than in others, exposing the slowest etching crystal planes as etch time progresses, usually the (111)planes of silicon. The ER dependence on orientation can be explained by the crystal structure of silicon (see next chapter). The typical etch rate is about $1\mu m/min$. Below is a scheme for both isotropic and anisotropic wet etching.

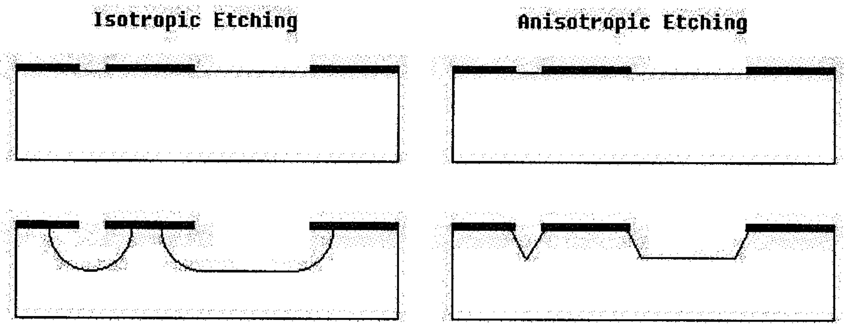

Figure 1–2: Comparison of isotropic (left) and anisotropic (right) etching as a function of time. The top ones are the substrates before etching, and the bottom ones are the etched pits in isotropic etchant and anisotropic etchant

Typical etchants for anisotropic wet etching are alkali hydroxide base, i.e. KOH, Ethylene Diamine Pyrochatechol(EDP), and tetramethyl ammonium hydroxide(TMAH). The reaction sequence is the following [7]:

$$Si + 2OH^- + 2H_2O \rightarrow Si(OH)_2^{2-} + 2H_2 \tag{1.1}$$

The silicon atoms are oxidized by OH^- and then removed from the substrate. As a consequence, the ER of silicon depends on the concentration of OH^- . That is to say, we can adjust the PH value of the solution to change the ER.

Due to the etch rate dependence of orientation, anisotropic etching is used to make V-grooves, silicon mesas and some free standing structures.

1.2.2 Dry Etching

Dry etching is a quite new technique. In this process, certain chemical or mixtures are driven into a low pressure chamber in the plasma phase, and then react with the sample chemically or physically [6]. The etching profile could be isotropic or directional, depending on the etching mechanism and the components of the chemicals [6, 8]. By adjusting the pressure or the component of the mixture in the chamber [9], we can use dry etching to etch most materials with a controllable ER. Often dry etching is usually used to pattern the top layer which is used as the mask for the following etching.

As mentioned above, the reaction mechanisms, reaction rates, chemistries and diffusion properties could be very different, so there exist many methods to do bulk micromachining. Table 1-2 provides a generalized comparison of various etchants in terms of many important properties [10].

Table 1–2: Comparison of Typical Bulk Silicon Etchants

	HNA	Alkali Base	EDP[1]	TMAH	XeF_2	DRIE[2]
Etch Type	wet	wet	wet	wet	dry	dry
Anisotropic?	no	yes	yes	yes	no	yes
Si ER(μ m/min)	1 to 3	1 to 2	0.02 to 1	≈ 1	≈ 1	>1
Si Roughness	low	low	low	variable	high	low
Nitride Etch	low	low	low	1 to 10 nm/min	-	low
Oxide Etch	10 to 30 nm/min	1 to 10 nm/min	1 to 80 nm/min	$\approx$ 1 nm/min	low	low
Al Selectivity	low	low	low	high	high	high
Au Selectivity	moderate	high	high	high	high	high
p++ Etch Stop	no	yes	yes	yes	no	no
Electrochemical Stop	-	yes	yes	yes	no	no
IC Compatible	no	no	yes	yes	yes	yes
Cost	low	low	moderate	moderate	moderate	high
Safety	moderate	moderate	low	high	moderate	high

1.3 Surface Micromachining

Bulk micromachining means that three-dimensional features are etched from bulk materials. In contrast, surface micromachined features are built up, layer by layer, on the surface of a certain substrate, e.g. a single crystal silicon wafer. Deposition and dry etching defines the surface features in the x,y plane and wet etching

[1] EDP: Ethylene Diamine Pyrocatechol.

[2] DRIE: Deep Reactive Ion Etching.

releases them from the plane by undercutting. Below is a typical process of surface micromachining to make a pressure sensor.

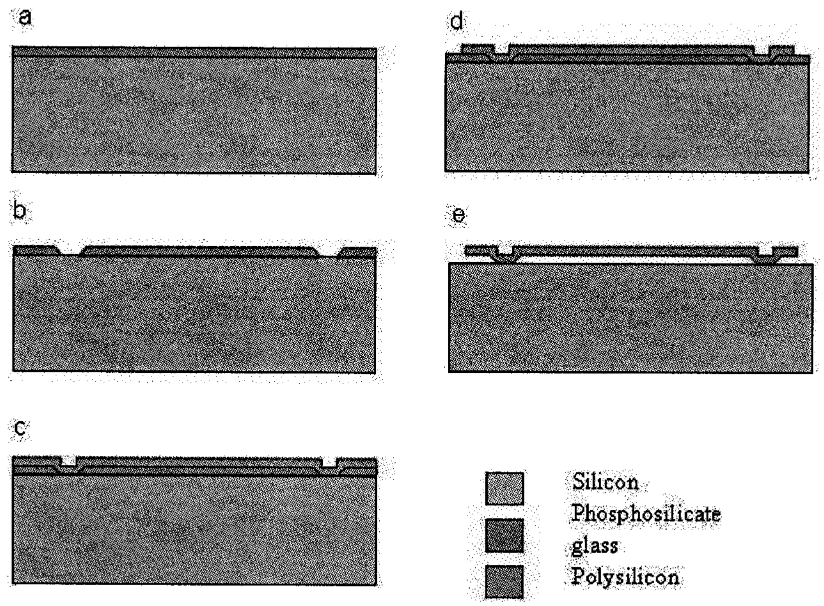

Figure 1–3: Typical surface micromachining process sequence to make a pressure sensor:a)Sacrificial layer deposition; b)Top side patterning; c)Device layer deposition; d)Device layer patterning; e)Selectively etching of sacrificial layer

From the process scheme, we can see that in surface micromachining, usually a sacrificial layer(Phosphosilicate glass in the diagram)and a structural layer(Polysilicon in the diagram) are needed, and the structural layer will be released by selective etching of the sacrificial material after patterning. That is why surface micromachining is also called sacrificial layer etch technique. The sacrificial layer could be silicon oxide, phosphosilicate glass and even photoresist. The mostly used and well studied structural material is polysilicon.

The great advantage of surface micromachining lies in the fact that, compared to the conventional bulk micromachining methods, mechanical structures with larger freedom in design can be built. The disadvantage is the restriction to thin films. Since the microstructure made by surface micromachining is often very thin, the stress, the hardness, the stiction and any other involved properties of the structural material should be taken into consideration in advance.

Besides the techniques used in bulk micromachining to pattern and release structures, many other methods are used in surface micromachining to grow or deposit a certain layer on the substrate. such as the growth of thermal silicon oxide. Chemical vapor deposition(CVD) and electron-beam-induced metal deposition are the most often used ones.

Surface and bulk micromachining have many processes in common. Both techniques rely heavily on photolithography, oxidation, diffusion and ion implantation, etc. Where the techniques differ is in the use of anisotropic etchants, anodic and fusion bonding, double-sided processing and etch stop in bulk micromachining, and the use of dry etching in patterning and isotropic etchants in release steps for surface micromachining. Surface and bulk micromachining are complementary techniques; combinations of both techniques are frequently used to fabricate complicated structures. The use of surface microfabrication avoids many challenging processing difficulties associated with bulk micromachining while bulk micromachining could help in integrating functional structures with a tiny chip.

CHAPTER 2
Wet Etching of Silicon in TMAH

In spite of the development of surface micromachining in the recent years, the bulk micromachining of silicon remains a quite important process in microfabrication, not only because of its widely use, but also its relatively well established facilities. Wet etching of silicon is used mainly for cleaning, shaping, polishing and characterizing structural and compositional features. Compared to dry etching, wet chemical etching provides a higher degree of selectivity, and is often faster. Referring to table 1-2, we can see that TMAH, as an anisotropic etchant, has many advantages, such as high selectivity to thermal oxide, very smooth etching surface, IC compatibility and easy to handle with high safety. Establishing this process of wet etching of silicon with TMAH was thus the first project of my M.Sc. Thesis.

2.1 The Crystal Structure of Silicon

Since TMAH is an anisotropic etchant, the structure etched in TMAH are usually formed by several special planes of silicon. In order to get a good understanding of TMAH etching, we should first know the crystal structure of silicon.

The crystal structure of silicon is that of the diamond type with lattice constant $a = 5.43\dot{A}$. The structure is face centered cubic(FCC) but with two atoms in the unit cell. The following figure shows the atom lattice of silicon and some facets of the silicon crystal.

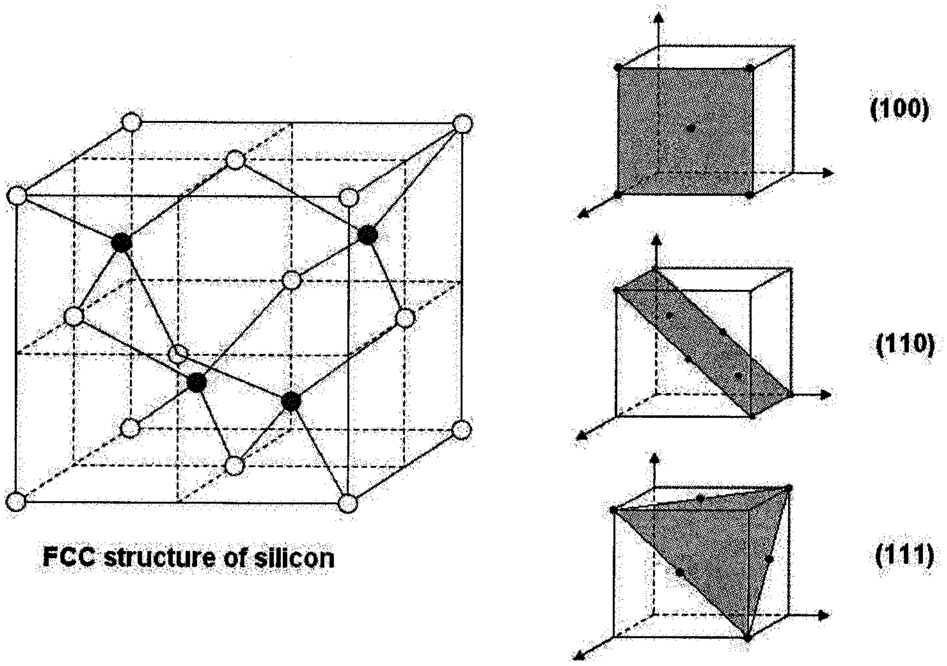

Figure 2–1: Fcc lattice of silicon. The right side are several special planes of silicon.

The commercially available silicon wafers are (100) and (110) wafers, depending on the orientation of the wafer surface. In research, the mostly used ones are (100) wafers. On this type of wafer, the surface is (100) so (111) planes make an angle of 54.74^o to the wafer surface.

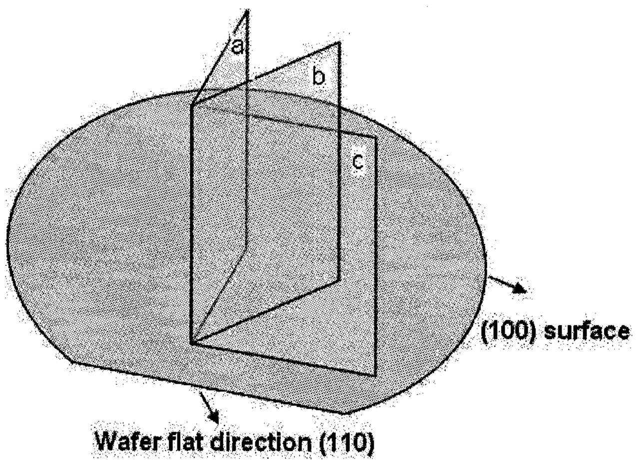

Figure 2–2: On a (100) silicon wafer, the surface is a (100) plane and the wafer flat is along the (110) direction. a, b, c are (110), (100), (110) planes respectively, and they are all perpendicular to the wafer surface

2.2 Etching Profile of TMAH

Similar to other anisotropic etchants, TMAH etching results in geometric shapes bounded by perfectly defined crystallographic planes.

2.2.1 TMAH Etched Structures

Figure 2-3 shows the diagram for the structures etched in TMAH with some opening. The top one is the mask I used, the bottom one is the pit after etching. (a) is an square opening which is along the (110) direction, (b) is also an opening along the (110) direction, but the size is smaller, (c) is another opening but now the edge is along the (100) direction, which is 45^o to the wafer flat.

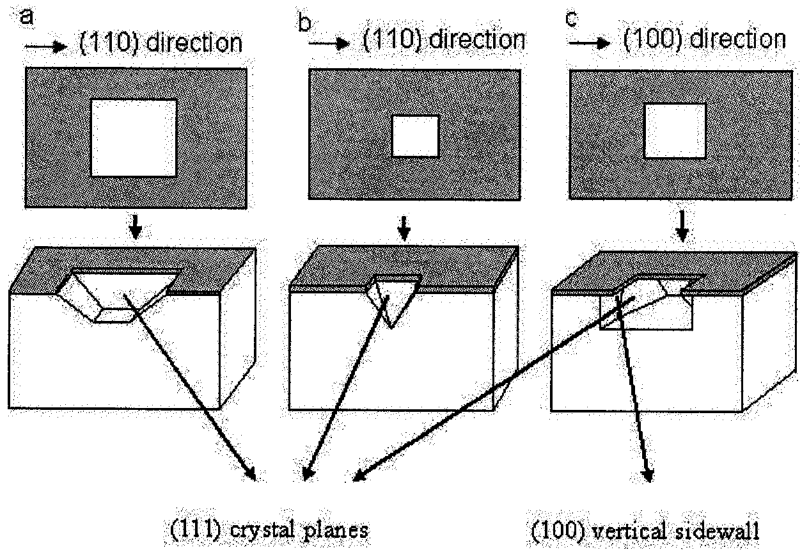

Figure 2–3: Diagram for TMAH etching. The top ones are the masks, and the bottom ones give the etched results. In case a, a big square opening whose edge is along the (110) direction is used. The sidewalls are the slowest etching planes-(111) planes and the bottom is a (100) plane. In case b, the mask is similar to that of case a, just the size is smaller, so those (111) planes meet together at the bottom, thus forming a pyramid shape. In case c, a rotated square is used, and now the edge is along the (100) direction. In this situation, the vertical (100) planes appear as sidewalls, and the (111) planes expose on the corners.

Figure 2-4 is a SEM photograph of the silicon wafer being etched in 25% TMAH at 85^oC, (note that unless otherwise specified, TMAH in the following text means 25% TMAH at 85^oC, the normal experimental condition used in our fab).

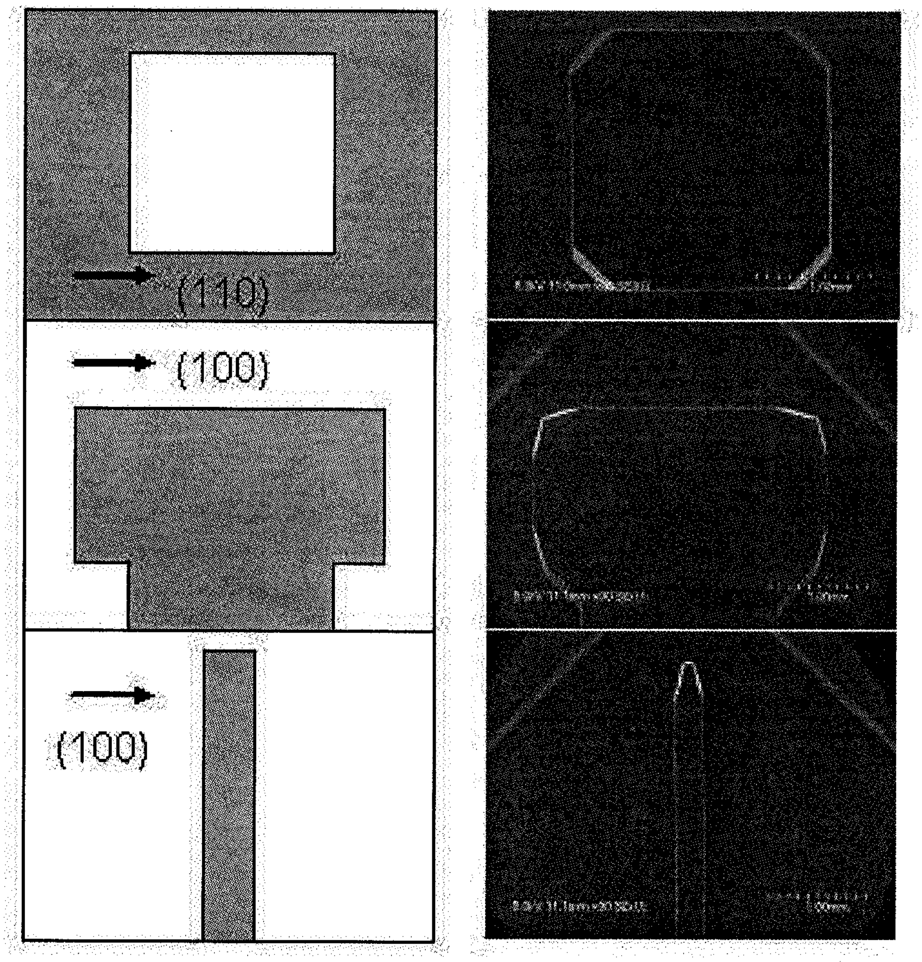

Figure 2–4: SEM Images of structure etched in TMAH. Left:mask shape; Right: SEM view of etched structure. The scale in the images is 1.00 mm

From the images, we can find that, the shape of the etched pit is not the same as the initial mask because of the undercutting and anisotropic etching. Due to the orientation dependent etch rate, the etched surface is composed of several crystal planes of silicon. By measuring the undercutting of the silicon, shown in the following figure, I found that the ER of (100) is about $0.48\mu m/minute$, and the ER of (111) is about $0.025\mu m/minute$.

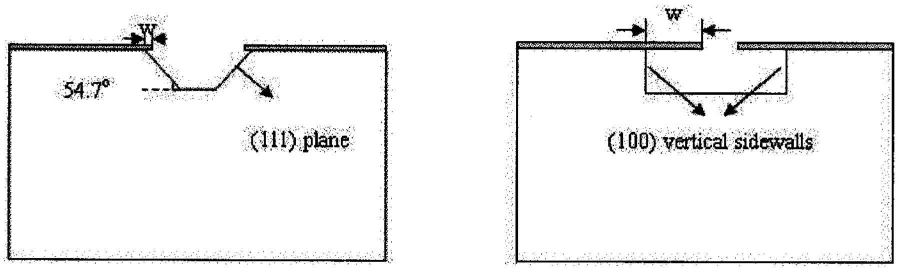

Figure 2–5: Undercutting under the mask:The ER can be obtained by measuring the undercut distance below the mask-"w" in the figure

These are the ERs for fresh 25% TMAH at 85^oC. It varies a lot with the experimental condition [11, 12], such as the temperature, the concentration, the agitation, even the neighbor facets [13, 14]. For example, with the decreasing of the concentration, the ER will be increased from $0.5\mu m/min$(25% TMAH at 85^oC) to $1\mu m/min$(5% TMAH at 85^oC) and increasing the temperature results in faster etch rate. The temperature and concentration influence is well studied [11, 12, 15], but the effects of the neighbor facets is still an object of research. And in my experiments, I found that the ER dropped down significantly after several wafer's etching, that is maybe because of the mixed product of the chemical reaction. The variation in ER is one of the biggest problem for the wet etching, and is still under examination. In order to get a better understanding of TMAH etching, I did two experiments. First, using the wagon wheel mask [15] to get the ER dependence of TMAH etching;

second, using a mask with different shapes of openings to determine the rules for TMAH etching.

2.2.2 Wagon Wheel Experiment

The wagon wheel method is developed to determine the ER under a mask that is aligned along a particular crystallographic direction of a wafer of a given crystallographic orientation. The idea is that many crystallographic orientations in the zone of the wafer orientation are exposed to the etchant, and one hoped to be able to extract the rate where the mask is underetched for all directions in the zone. For example, to measure the ER of the (111) plane, we make an opening along the (110) direction which is the intersection line of the (111) plane with wafer surface, and measure the undercutting of the silicon substrate after a certain time in TMAH. In order to get the ER of different orientations, a mask consisting of many spokes along different orientations is designed, as shown in the following picture. This method is the wagon wheel method.

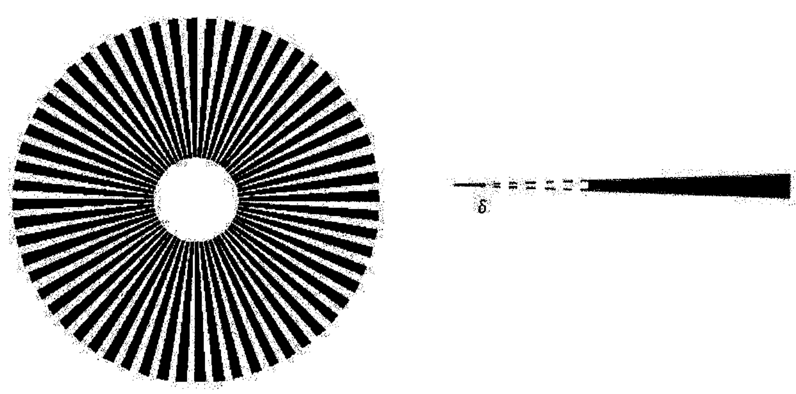

Figure 2–6: Mask patten for the wagon wheel method. It consists of many spokes which are along different direction and have an angle of δ.

Using this kind of mask, we need to take a SEM view of the cross section of every spoke, which is time consuming. Besides, since the ER of the (111) plane is very slow, the underetch of such planes is small, therefore the experimental uncertainty is large. To overcome these problems, Seidel [7] suggested a mask pattern in a form similar to a wagon wheel. In this mask, the masked regions have the form of long isosceles triangles in place of wagon wheel spokes. The spokes have a width of δ, and are separated by θ. The following picture shows the detail of one of the spokes after undercutting in TMAH(in the figure the angle is enlarged).

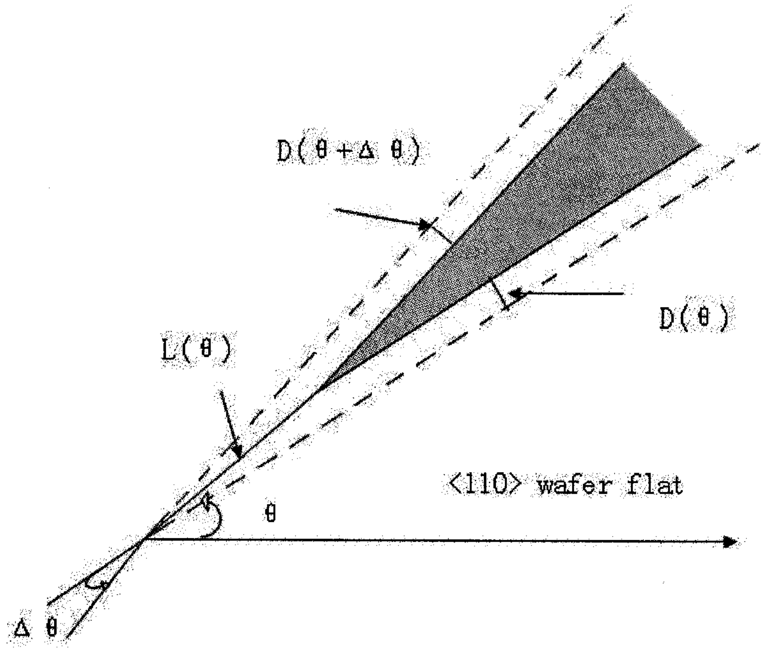

Figure 2–7: Detail of the wagon wheel mask:The dashed line is the outline of the original shape of one of the spokes in the improved wagon wheel mask. The shadowed part is the result after TMAH etching. $L(\theta)$ is the distance from the original apex to the apex after etching. $D(\theta)$ is the undercutting of the crystal sidewall. $(\Delta\theta)$ is the angle of the isosceles triangle spoke.

The mask is undercut from both sides by a distance $D(\theta)$ and $D(\theta + \Delta\theta)$, respectively, and the underetch fronts intersect each other at a distance $L(\theta)$ to the sharp end of the original spoke. If we ignore the underetch in the direction of the long axis of the spokes(along L)(often neglectable) and the difference between $D(\theta)$

and $D(\theta + \Delta\theta)$, we have a simple relation between L and D,

$$D = Lsin(\Delta\theta/2) \approx L\Delta\theta/2orL \approx 2D/\Delta\theta. \tag{2.1}$$

In this case, the measurement L is enhanced by factor $2/\Delta\theta \approx 115$ for $\Delta\theta = 1^o$. The wagon wheel pattern makes anisotropic etching easily visible, and minute underetching of the spokes results in large, easily measurable undercutting in a radial direction. In my experiment, I used $\Delta\theta = 1^o$, and the separation of the spokes is 1^o. The following picture is the photo of the wagon wheel pattern on a 6 inch wafer after 4 hours in TMAH(It was taken with a digital camera, and due to the reflectivity and shininess of the surface, it was not very clear.)

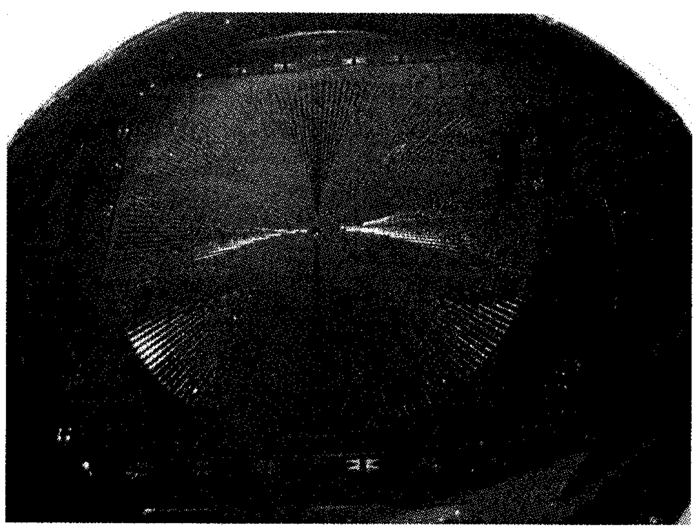

Figure 2–8: The result of the wagon wheel experiment. The wagon wheel has a diameter of 76 mm, and the substrate is a 6 inch wafer. Though it is not very clear, we can obviously see the dependence of the ER on orientation.

In order to get a SEM image of it, I did the experiment again but this time, the wagon wheel pattern was resized by the stepper(The stepper is used to transfer the pattern on the mask to the substrate with a ratio of 5:1). Now the diameter of the wagon wheel was 15.2 mm, and it was put in the TMAH for 40 minutes. Below is a SEM image of part of the wagon wheel.

Figure 2–9: SEM view of part of the wagon wheel. The island on the left corner is the center of the wagon wheel[1] , and the bottom of the image box is along (110) direction.

[1] The island is caused by the resolution of the mask. Since many spokes meet at the center, the printout of the mask design will be limited in quality in the center part(see appendix A for the mask making).

The undercutting in the radial direction cannot be completely ignored though it is small compared to L due to undercutting of both sides of the spoke, for example, it is about 120 μm while $L \approx 2D/\Delta\theta = 1,800\mu m$ for $\theta = 45^o$ after 30 minutes in TMAH. The edge is a convex corner which will be bound by fast-etching planes(This will be discussed in the following section). Therefore, really reliable underetch rates can be only obtained by measuring the undercutting D directly.

The disadvantage of this technique is two fold. The first problem is trivial: the undercutting rate is determined for discreet orientations, therefore a higher resolution of the underetch rate as a function of the orientation requires more spokes, which means a high resolution mask is needed. The second problem is more serious. The pattern that is seen on the top of the wafer is only a projection of underetch rate on the wafer surface, (100) plane. We can not tell the exposed crystal planes just by the direction of the intersecting lines with the wafer surface. To solve this issue, people used a silicon sphere to give complete information about the ER of the etchant [16].

From the result of wagon wheel experiments, we can get some important information about the TMAH etching. The slowest etch plane occurs on (111) crystal plane. Lots of conflicting data can be found in the literature on the fastest etch plane. Many planes are reported to be the fastest etch planes, such as the (212) plane [17], or the (411) plane [18]. In my experiment, the fastest plane occurs at the spoke which is 30^o to the wafer flat. It is almost the same as the angle between the intersecting line of the (411) plane with the (100) surface, which is $45 - arctan(1/4) = 31^o$. So in this thesis, I take the (411) plane as the fastest plane. Besides the maximum and minimum ER orientation, there is a local minimum in the ER profile of TMAH, the

(100) plane. Since the (100) planes are normal to wafer surface, it is quite useful in some situations.

The ER ratio of the (111) plane to the (100) plane for 25% TMAH at 85^oC is about 1:20. This number indicates the degree of anisotropy of the etchant. There are many models to explain this anisotropy [7, 19], however, quantitative understanding of the chemical mechanism of silicon wet etching would be of invaluable help in writing more predictive silicon etching software code.

2.2.3 Prediction of TMAH etching

As seen previously, the etched structure is very different from the original mask that is used, such as, the square opening ends up with (111) planes as the side walls and the corners of the rectangular pad will be rounded off very much after the TMAH etching, see figure 2-4. To get more information about the TMAH etching, I designed a mask with different opening shapes. These openings consist of many corners whose edges are along different directions. Figure 2-9 is a part of this mask.

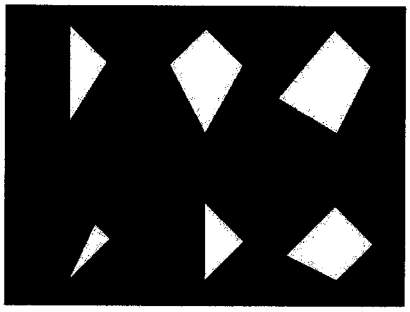

Figure 2–10: Mask used to get more details about the TMAH wet etching of silicon. Many openings whose edges are along different directions are included. The purpose is to find the principle of TMAH etching so that we can use this knowledge to design the proper masks.

I patterned a silicon wafer using this mask, and did a 6 hours' TMAH etching, then I viewed the sample under SEM. I found that, for a concave corner, besides the planes parallel to the edges of the corner, the etched pits were dominated by slowly etching planes, mainly (111) planes and sometimes (100) planes; and for a convex corner, the structures were then dominated by the fast etching planes. In my case it is (411) planes. The results are shown in the following picture.

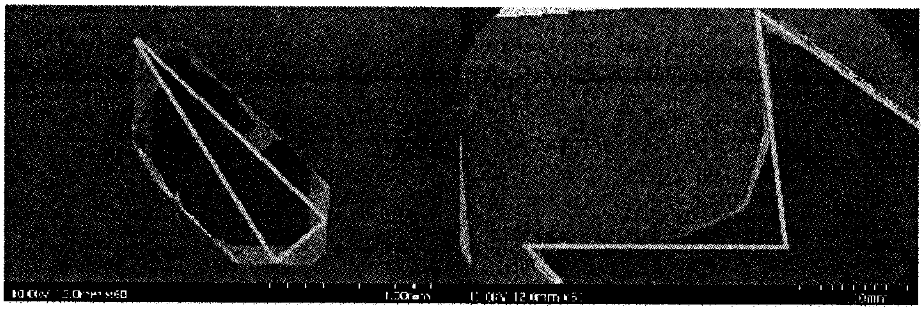

Figure 2–11: Etching results of the mask used in figure 2-10. The left one shows the result of concave corners and the right one is the undercutting of a convex corner. The superimposed line indicates the shape of the mask used to pattern the surface. On the left image, we can see some hanging films on the edge with irregular shape. This is the oxide film residue which is used as the mask and it can be easily removed in diluted HF without attacking silicon. The scale is 1.00 mm, and the SEM parameters are, voltage-10.0kV, working distance-12.0 mm, magnification-X50.

These facts will cause some problem when we want to etch deep into the substrate because the etched pit will be quite different from the mask that we used. For example, the following picture shows the result of a mask opening of arbitrary shape caused by the undercutting.

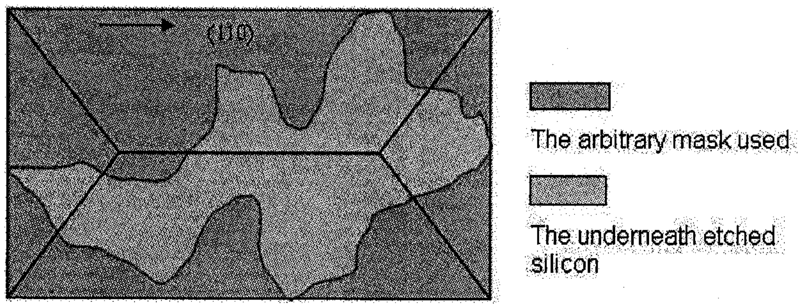

Figure 2–12: Since the (111) planes are almost not attacked by the solution, the etched structure of an arbitrary opening will be formed of (111) planes after a long time's etching in TMAH, no matter what kind of opening it is.

On the other side, the undercutting could be helpful in designing some structures, especially in making a freestanding structures.

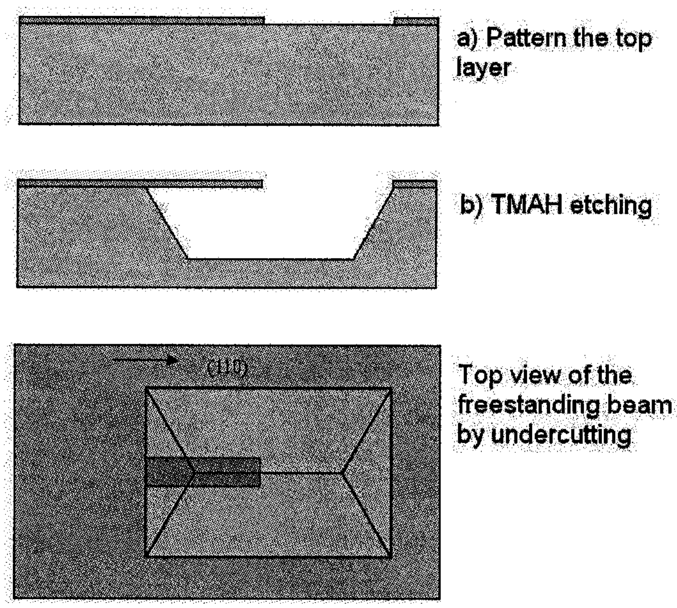

Figure 2–13: Freestanding beam made by undercutting

2.3 Etch Stop Technique

The use of etching to shape objects is not of much help if one is not able to control the depth and width of the etched dimension. The lateral dimensions, sometimes can be defined by the slowly etched (111) plane if we let the edge parallel to the (110) direction. For example, V-grooves, which are used to place a fibre, can be etched using a rectangular opening whose edge is along (110) direction. Since the etched front will be bounded by (111) planes, the etched pit will almost remain the dimensions of the mask. We just need to make the size of opening a little bit smaller to compensate the etch of these slowest etching planes. The depth of the V-grooves can be controlled by the width of the openings.

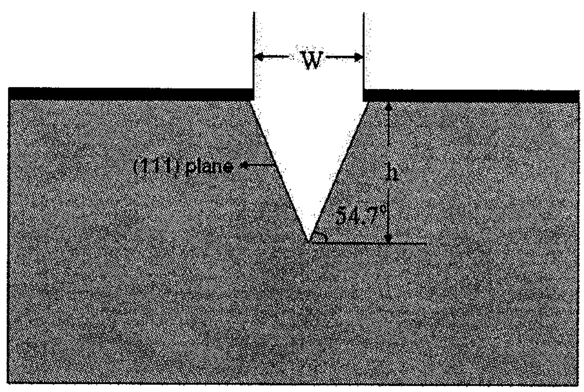

Figure 2–14: Using a V-groove as an etch-stop. The etched depth is well defined at the exact moment when the v-groove is formed.

Since (111) planes make an angle of 54.7° to the wafer surface, there is a relation between the etch depth to the width of the opening, that is

$$w = 2\sqrt{2}h \tag{2.2}$$

For example, if we want the etch depth to be 50 μm, the width of the opening should be $2\sqrt{2}50 = 141\mu m$. At the precise moment the V-groove is developed, the etched depth has reached the desired one. This technique is suitable for making V-grooves like structure, but when we want to use this method as an etch stop to help making some other kind of structures, such as a membrane of certain thickness, or a pillar with certain height, it is difficult to get a precise result, because it is difficult to tell the exact moment when the V-groove is formed. For large V-grooves, and not precise situation, we can tell it by just observing it using our eyes, but in most cases, it is not accurate enough. Although Nunn and Angell [20] claimed that an accuracy of about 1 μm could be obtained using the V-groove method, none of the mentioned techniques are found to be reliable and production worthy. So we need some other etch stop techniques to do this. The following possibilities are used.

2.3.1 Time Controlled Etch Stop

The time controlled etch stop is the most trivial way to stop the etching. The wafer is removed from the etchant after a given time of etching. The time is calculated by the ER of the etchant. The obvious advantage is the simplicity of this procedure, and the use of timing technique is acceptable when we are not very demanding on the dimensions, usually sizes greater than 50 μ m.

However, it is not accurate. There are many reasons for this. At first, as mentioned before, the ER of TMAH is hard to keep constant during the whole processing time. Secondly, the roughness of the surface is around 1 μ m, which is a problem when we need a smooth surface.

Despite the inaccuracy of timing technique, it is useful in estimating the processing time.

2.3.2 Boron Etch Stop

Due to the shortcoming of the timing technique, a boron etch stop is a widely used etch stop mechanism nowadays. It is based on the fact that heavily boron-doped silicon was etched much slower than low doped silicon. [21, 22]. At a boron concentration around $2 \sim 3*10^{19}cm^{-3}$, the ER starts to slow down. The decrease of the etch rate is nearly independent of the crystallographic orientation, and the critical concentration at which the ER starts to decrease is slightly temperature dependent.

The boron doping can be done by ion implantation or gas phase deposition. We can use a silicon oxide layer as the mask to selectively dope the silicon wafer with boron [21]. The following figure shows a typical process of making a membrane using a boron etch stop technique.

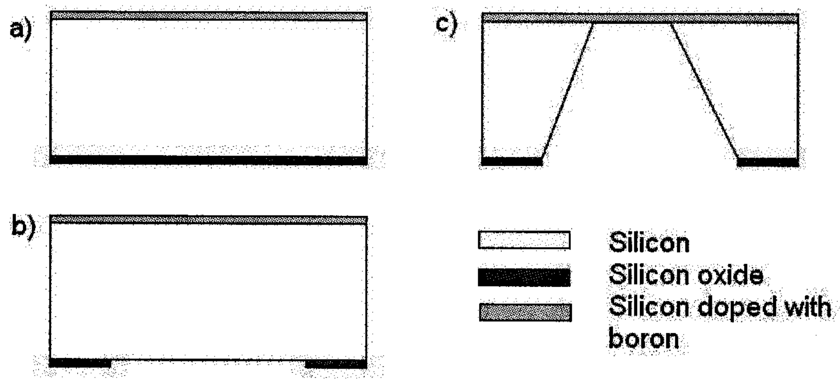

Figure 2–15: A typical process of making a silicon membrane using the boron etch-stop technique. Step a: Dope the top side with boron. The depth of the doped layer can be controlled by the energy of the implanted boron. Step b: pattern the backside oxide. Step c: TMAH etching.

Compared to the timing technique, it has more accuracy and is easier to handle. However, since boron atoms are smaller than silicon, it will cause stress in the membrane or beams we get. Also the conductivity of silicon is greatly enhanced by dissolving boron in silicon. The material is no longer suitable for electrical purposes, and indiffusion of resistors is no longer possible. Another issue is that, it is much expensive than the timing technique. normally, it costs 400-500 Canadian dollars to dope a single 6 inch wafer.

2.3.3 SOI Wafer Used as Etch Stop

Anisotropic etching solutions do not attack a great number of materials. Hence, a thin film of such material can be used as an etch stop. Silicon on insulator (SOI) wafer is such an example. The following is a scheme for the SOI wafer.

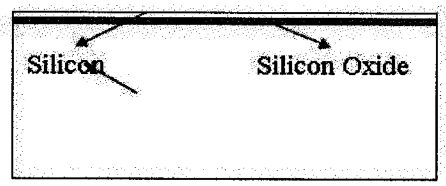

Figure 2–16: SOI wafer. The top silicon layer is usually called device layer. Tho bottom silicon substrate is called the handle part.

SOI wafer can be made by oxygen implantation or wafer bonding , the top silicon layer is the device layer while the bottom layer is often used as the handle. The buried oxide layer is not only used as the etch-stop in the wet bulk etching, but also becomes an insulator between the top silcon and the bottom silicon layer. Since there is no boron doped in the silicon in SOI wafers, it gets rid of the stress and conductivity problems. Similar to the boron doping technique, it is expensive too. Normally, the price of a SOI wafer is 300 CAD while a regular wafer is only 20 CAD.

Besides the above mentioned methods, electrochemical etch-stop techniques are also used [6]. It involves doping and biasing of silicon during anisotropic etching. The advantage is that low doping levels are sufficient for the etch stop; therefore microstructures machined with this method still are suitable for integrated circuits, and there is no problem with stresses. The disadvantage is that the method is much more complicated than the boron etch stop

2.4 Mask Materials

In principle, all materials that are etched slowly enough in TMAH are suitable for mask materials. The choice of a particular mask material depends on a number of considerations. The main issues are availability in the lab, ease of the process(such as processing time, complexity of the process and reliability), selectivity of the etch process with respect to silicon, and costs. Of many materials, silicon dioxide and silicon nitride are the mostly used ones.

2.4.1 Silicon Dioxide

Silicon dioxide, SiO_2, is probably the most important mask material in microfabrication. There are many advantages of silicon dioxide.

First of all, it can be grown on silicon wafers easily by oxidizing the wafers. Two basic schemes are used: wet and dry oxidation.

Wet oxidation: $Si(s) + 2H_2O(g) \rightarrow SiO_2(s) + 2H_2(g)$

Dry oxidation: $Si(s) + O_2(g) \rightarrow SiO_2(s)$

Here s and g means solid and gas respectively.

Silicon dioxide growth involves the heating of a silicon wafer in 1 atm stream of wet or dry oxygen at elevated temperatures (between 800 and $1,200^0C$) for several hours. The processing time depends on how thick the oxide is needed. The oxidation rate depends on such parameters as crystallographic orientation of Si, the temperature in the furnace, the processing time and even the thickness of native oxide on the wafer. There are many papers giving the mechanism of the thermal oxidation of silicon and the prediction of the thickness in terms of processing time and temperature [23]. Wet oxidation is faster than dry oxidation process, for example, to grow 0.4 micron oxide on a blank (100) silicon wafer at $1,000^0C$, wet oxidation needs one hours, while dry oxidation needs almost one whole day, however, the quality of silicon dioxide by dry oxidation is better than that of wet oxidation. In spite of this, wet oxidation is preferred in many cases because it is good enough to be used as the mask layer,.

Another thing should be considered here, that is, during the oxidation, the silicon will be consumed. The ratio of silicon thickness converted, X_{si}, to resulting oxide thickness, X_{Oxide}, is proportional to their respective densities: $X_{Si} = 0.46X_{Oxide}$. This should be take into consideration when we are strict on the remaining thickness of the silicon.

Secondly, the selectivity of silicon dioxide to silicon in TMAH is very good. SiO_2 etch rate is 4 orders of magnitude lower than (100) Si [6]. That is too say, to etch through a 6 inch wafer, which is 675 μm thick, 1000 $\dot{A}$ oxide film is enough. Actually, in order to make sure the silicon underneath will not be attacked, we usually use slightly thicker oxide film.

Thirdly, silicon dioxide can be patterned easily using reactive ion etching(RIE) in a CF_4/O_2-based plasma.

Finally, silicon dioxide can be removed using wet etchant, such as diluted HF solution. The etch rate in 10:1 H_2O to HF is about 300 $\dot{A}$/min. So we can use buffered HF to release the etched structures.

2.4.2 Silicon Nitride

Silicon nitride can be grown on the silicon wafer through a CVD method, either by low pressure chemical vapor deposition(LPCVD) or plasma enhanced chemical vapor deposition(PECVD). Compared to silicon dioxide, it also has the high selectivity to silicon in TMAH, and can be patterned using RIE. The disadvantages are, the cost is higher and it is hard to remove using wet etching.

Besides silicon dioxide and nitride, nowadays, silicon carbide is emerging as a new material for microfabrication, not only be used as a mask layer, also be used as the structural layer [24, 25].

CHAPTER 3
Corner Compensation and Simulation

As seen before, the etched pits are usually quite different from the mask we used because of the undercutting, especially at the corners of the structures. In the following optical image, we can see obviously the rounding off of the corners due to underetcutting of the uncompensated mask.

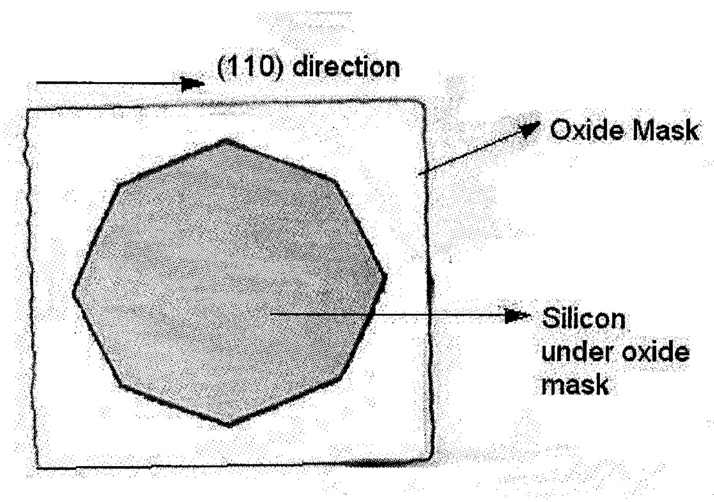

Figure 3–1: The optical image of the undercutting of convex corners. The oxide mask is a $80\mu m$ by $80\mu m$ square, and the etch time is 40 minutes.

If the etching depth is small and the x-y dimensions of the structure are much larger than the etching depth, the undercutting will not cause a big problem. This is always the case in surface micromachining. However, when we are doing bulk micromachining, we need to think about the effect of underetch. For example, in order to make a square mesa, which is 300 μm by 300 μm large, and 300 μ m high, we need to put the wafer in TMAH solution for 10 hours (here I use the typical ER of TMAH, 30 μm per hour). If we use a 300 μm x 300 μm square as the mask, and the fastest etch plane (411) will emerge due to the undercutting. The intersection line of (411) and (100) makes an angle of 31^o to the wafer flat, showed in the following picture.

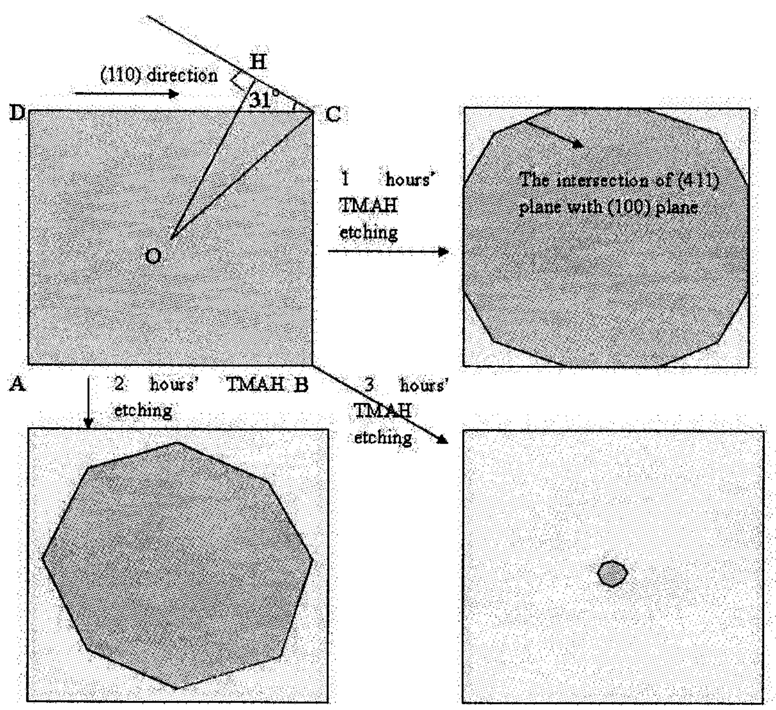

Figure 3–2: Disappearance of the silicon under the oxide mask due to undercutting. a)a 300*300μm square mask; b)60 minutes in TMAH; c)120 minutes in TMAH; d)200 minutes in TMAH.

$$AB = BC = CD = DA = 300\mu m \tag{3.1}$$

$$OC = 300/\sqrt{2} = 212\mu m \tag{3.2}$$

$$OH = OC\sin(45+31) = 206\mu m \tag{3.3}$$

Since the ER of (411) plane is about 60 μm per hour(the projection of the ER of the (411) plane on the wafer surface), it only needs $\frac{OH}{60} = 3.4 hours$ to etch all the silicon under the mask away, and nothing will remain after 10 hours' etching in TMAH. So it is important to take the undercutting into consideration if we want to get sharp corners.

3.1 Methods for Corner Compensation

It is possible to compensate for the undercutting of convex corners by a suitable mask design [26].

3.1.1 Triangle strips

Since the undercutting is caused by the etching of the fastest planes, the trivial thought is to include triangle strips on the corners of the mask, shown in the following figure, the sides of the triangle, e.g. BC, is along the intersection line of (411) with (100).

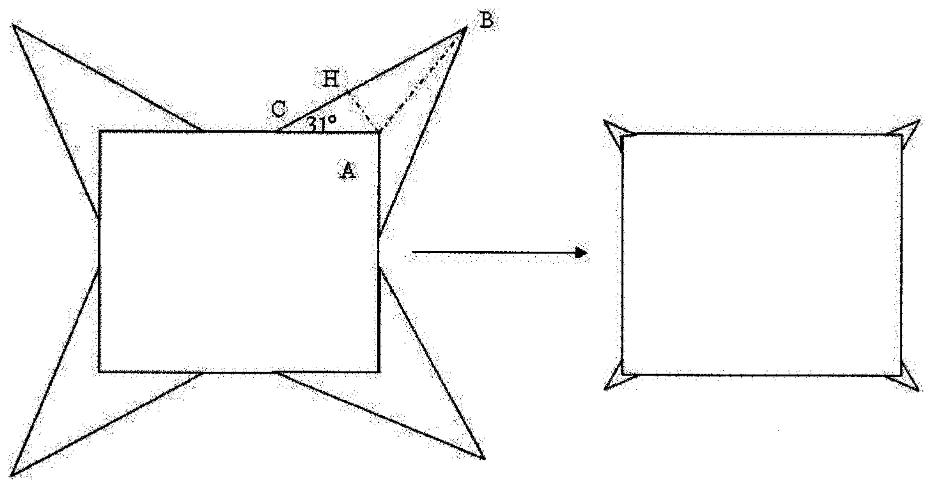

Figure 3–3: Triangle strips as the corner compensation. Left: mask used; Right: result after etching

The fast etching planes start to erode at convex corners. But the final convex corner is protected by this sacrificial structure so that after the compensation structure has been etched away, a rectangular corner remains. The dimensions of the adding structures should be carefully designed according to the ER and etch time. If the etch depth is h, then

$$Etch\ time\ T = \frac{h}{ER(100)} \tag{3.4}$$

$$AH = ER(411) * T \tag{3.5}$$

$$AC = \frac{AH}{\sin(31^o)} = \frac{ER(411) * h}{ER(100) * \sin(31^o)} \tag{3.6}$$

$$AB = \frac{AH}{\sin(14^o)} = \frac{ER(411) * h}{ER(100) * \sin(14^o)} \tag{3.7}$$

For example, to get a square mesas of size 1 mm by 1 mm and with a height of 100 μm, the dimension of the triangle strip is

$$AC = \frac{ER(411) * h}{ER(100) * \sin(31^o)} = \frac{60 * 100}{30 * \sin(31^o)} = 388\mu m \tag{3.8}$$

$$AB = \frac{ER(411) * h}{ER(100) * \sin(14^o)} = \frac{60 * 100}{30 * \sin(14^o)} = 826\mu m \tag{3.9}$$

From here, we can see, if the etch depth is larger, the triangle strips need to be very big. For example, if the height of the mesas is 200 μm, then AC = 776 μm. Now, the edge of the square is not long enough to accommodate those strips($2AC = 1,552\mu m > 1,000\mu m$). This will clearly lead to a serious limitation of the density of mesas.

Another problem is that, the above picture is just a 2D view of the etched structure. The 3D structure could be quite different since the etch of those strips will leave some tails on after the desired period of etching. This can be seen clearly from the figure 3-5, 3-6 (although the corner compensation technique in those pictures are different from the technique used here, the same issue happens).

3.1.2 Strips along (110) direction

The strips oriented along the (110) direction can also be used as compensation for convex corners.

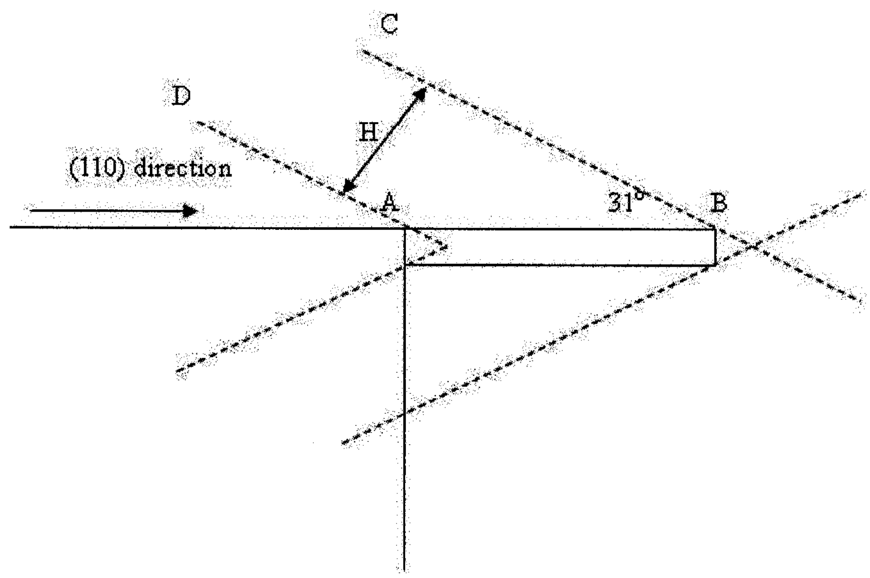

Figure 3–4: Strips oriented along the (110) direction as corner compensation

Since the (111) planes is etched very slowly in TMAH, the width of the beams almost remains the same during the etching. If the etch depth is h, then

$$Etch\ time\ T = \frac{h}{ER(100)} \tag{3.10}$$

$$H = ER(411) * T \tag{3.11}$$

$$AB = \frac{AH}{\sin(31^o)} = \frac{ER(411) * h}{ER(100) * \sin(31^o)} \tag{3.12}$$

In this method, to get a square mesas of size 1 mm by 1 mm and with a height of 100 μm, the length of the beams should be

$$AB = \frac{ER(411) * h}{ER(100) * \sin(31^o)} = \frac{60 * 100}{30 * \sin(31^o)} = 388\mu m \qquad (3.13)$$

The width of the beams doesn't need to be large as long as it can survive after the TMAH etching, that is to say, the width should be bigger than $2{*}ER(111){*}Etchtime$. Usually, it should be as small as possible to reduce the size of the residue on the corner formed by (411) facets. Below is the result of using 550 μm strips as the corner compensation. The etching time is 4 hours.

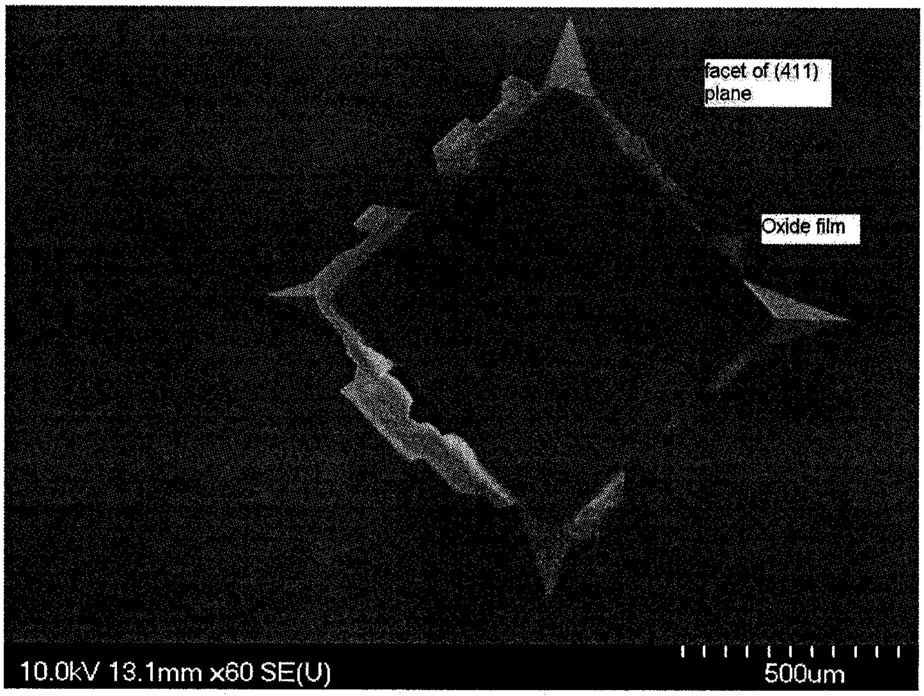

Figure 3–5: Result of using (110) strips as corner compensation. The strips used were 550 μm in length and 100 μm in width. The features along the edge of the square were the broken oxide film.

We can also see that there are some residue on the corners caused by the strips.

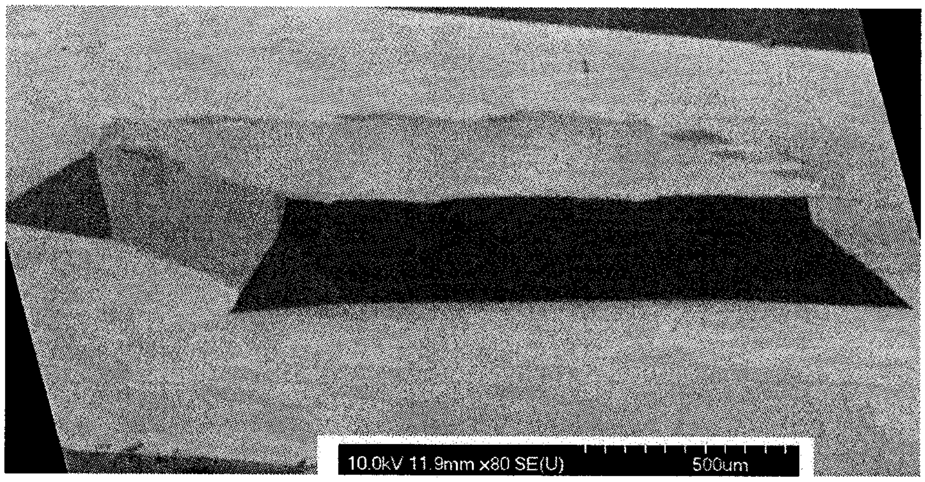

Figure 3–6: Tails on the corners using (110) strips as corner compensation

The disadvantage of strips along the (110) direction is also that it takes lots of space to include the corner compensation if the etch depth is large. For example, to etch through a 6 inch wafer, which is 675 μm thick, the length of the beams should be $388 * 675/100 = 2,600\mu m$. This can be solved using folded strips in a certain extent [27], as shown below.

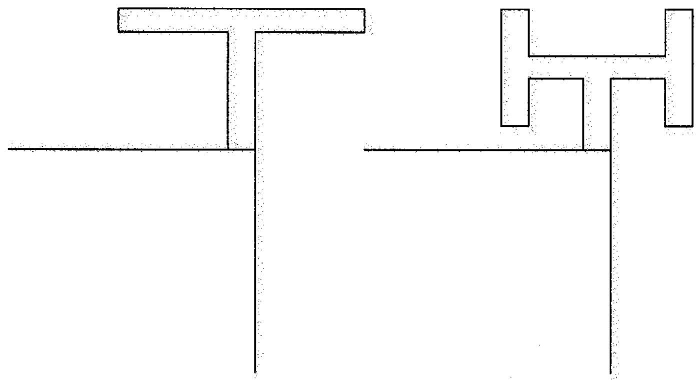

Figure 3–7: Folded (110) strips as the corner compensation. More than one turn could be used.

It works in the same way as the straight beams, just the length of the beams is a little shorter, and now it depends on the width of the beams. The following picture show the results of undercutting in 25% TMAH (not fresh solution) for 5 hours using the folded strips. The etch depth is 94 μm, and the length of the (110) strips is 1,200, 1,100, 1,000, 900, 700 μm respectively and the last one is the result of not using any corner compensation.

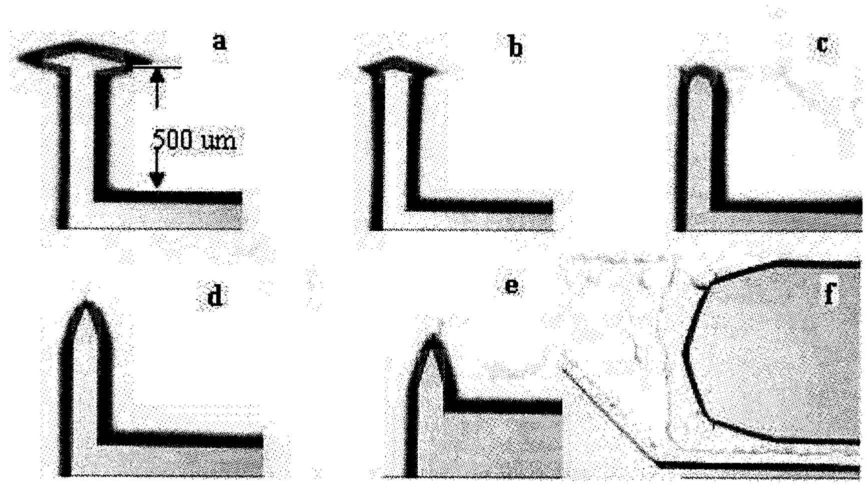

Figure 3–8: Optical images of the results using the folded (110) strips as the corner compensation. The length of the strips is a 1,200 μm, b 1,200 μm, c 1,200 μm, d 1,200 μm, e 1,200 μm, f no corner compensation. The transparent part superimposed on those strips is the oxide mask.

It is also possible to use more than one turn as corner compensation, as shown in the right part of figure 3-6. However, the folded strips should be designed with symmetry, the following design will not reduce the undercutting properly.

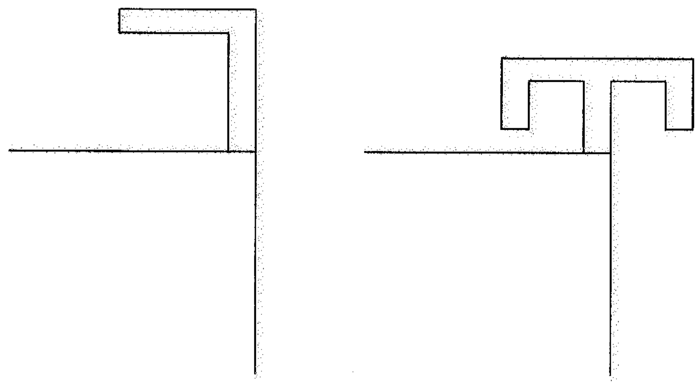

Figure 3–9: Incorrect mask design for corner compensation

3.1.3 Strips along (100) direction

Another method for corner compensation is to use strips in the (100) direction. The design of these strips is much easier than that of (110) strips. If the etch depth is h, then the width of the strips is $w = 2 * h$. To avoid the undercutting of the beams from the end of the beams, they can be connected to the external mask, as shown in the following figure.

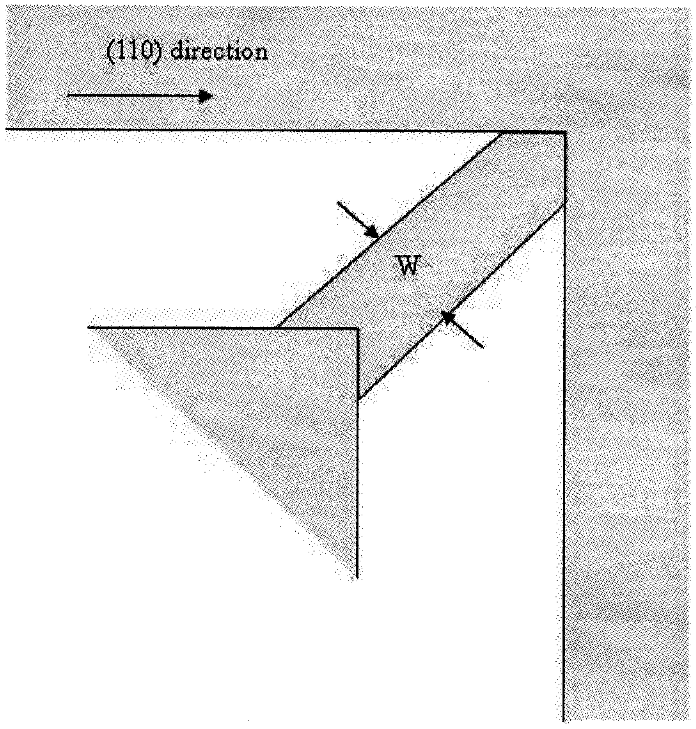

Figure 3–10: Strips oriented along the (100) direction as corner compensation. The width of the beam should be twice the etching depth.

The advantage of the (100) strips is that the compensation structure is mainly undercut by (100) planes and not by (411) planes, and because (100) planes are normal to the wafer surface, there are no extra residue remaining after the etching. And also, since the width is only two times that of the etch depth, it does not need large space to include the corner compensation. The only limitation is that it can not be used for small structures. For example, if the mesas required is only $200\mu m$ * $200\mu m$ large, and $100\mu m$ high, then the width of the (100) strip should be $200\mu m$. This is too big as two adjoint strips will intersect with each other, see figure 3-11.

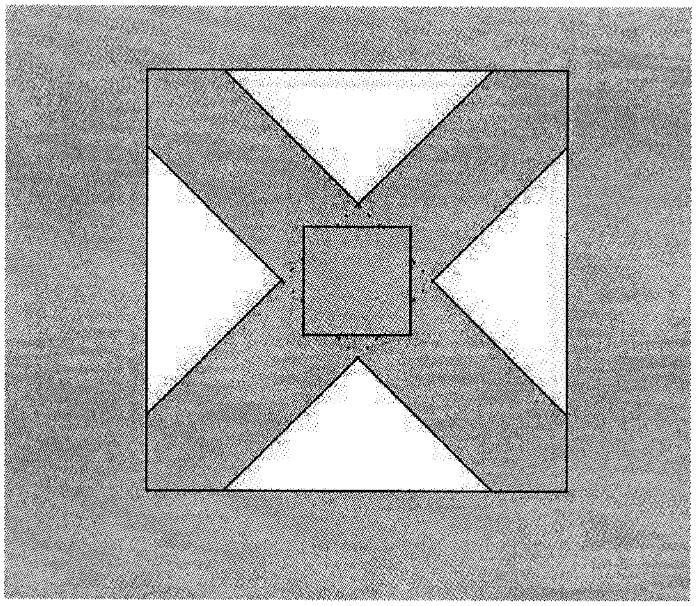

Figure 3–11: Strips are too wide for the corner compensation

Mayer has introduced adjusted (100) beams to solve this problem [28].

However, no matter what kind of compensation is used, timing is the difficult part: if etching is stopped too early, a peak remains on the corner while overetching leads to a structure with an undercut corner, similar to the non-compensated case but with less undercut. And as said before, the fastest etching plane depends on many factors, it is thus hard to accurately compensate. Nevertheless, corner compensation greatly improves the etched structure.

Compared to the convex corners, the corner compensation for concave corners is usually more difficult and the mask used is more complicated [29] because it is impossible to get rid of the (111) planes during the anisotropic wet etching.

3.2 Simulation for the Wet Etching Process

In order to make a desired structure, one always needs careful design of the mask, especially when we need to take corner compensation into consideration. For simple cases, like squares and grooves, we can calculate it and image it in our brain, however, if the structure is very complicate in 3D, and the mask needed has a more complex form, we should let the computer do the job. It will greatly shorten the processing time if we have a good simulator for the wet etching process because we can adjust the designing of the mask after applying it in the simulator, instead of trying it in the fab.

Many groups in the world are doing researches on the simulator [30, 31]. Methods for simulating the etching process fall into two categories: Cellular Automata (CA) method [32] and geometric method [33, 34, 35]. For the cellular automata method, it needs the knowledge of the mechanism of the silicon crystal and the interaction between the etchant and silicon. In this method, the computer records all the silicon atoms, especially those exposed to the etchant. Since each atom on the outside surface is on a different crystal planes and has different interaction with its neighborhood atoms, it requires different energy to break those Si-Si bonds and remove the atom from the substrate. So that, when an etchant molecular hits a silicon atom, there is a probability to etch the atom away. This probablity is determined by the strength of chemical bonds and the link status of its lattice neighbors, in the form of $exp(-\Delta E/k_B T)$ [32], here ΔE means the energy required to break the bond, k_B is the Boltzmann constant and T is the temperature. Experimental ER ratios as well as the influence of temperature and concentration of the etchant are taken into account by introducing a stochastic component. For example, from figure 2-1, we can see that, the silicon atom on the (111) surface has 3 neighborhood atoms beneath the (111) plane while the silicon atom on the (100) plane only has two neighbors under the plane, so the energy needed to remove the (111) atom is larger than that to remove the (100) atom. In the cellular automata model, this means the probability of removing the (111) atom is smaller than that of removing the (100) atom.

Since it records all the atoms, the CA method typically requires much computer memory and always deals with small dimensions of silicon substrate. Nonetheless, it exhibits high efficiency and accuracy when handling arbitrarily complex mask shapes and merging of three-dimensional structures.

In the geometric method, the silicon substrate is treated as a continuous entity, all the information needed is the ER profile of the TMAH that have been obtained experimentally, usually by the wagon wheel method and then using the rules of the TMAH etching to determine the evolution of the etching shape with time. It is much faster than the CA method, but since the ER of the etchant varies a lot with the experiment condition and the data for the ER most come from the wagon wheel method, it only gives a 2D diagram for the ER profile, so it is not that accurate as the CA method, and in order to include the temperature effect, it needs to reestablish the ER database However, in most cases, it is good enough to give an idea about the etching results under a certain mask.

3.2.1 Geometric Simulation

The principle I used to do the simulation is simple. That is to find those slowest or fastest etch planes for each corner. The slowest etching plane is the (111) plane, and it will come out in the concave corners. The fastest etching plane is the (411) plane, and it is for convex corners. Given an arbitrary corner, we human beings can easily find those special planes, but for the computer, it is not an easy job.

To Distinguish from a Concave Corner and a Convex Corner

Since different rules will applied when dealing with convex and concave corners, the first thing of the program is to tell the computer to judge if a corner is a concave one or convex one. In my program, I tell the computer to do this by the following method.

First, in order to tell the computer the shape of my mask, I input the coordinates of the apexes in order. Usually in the way that, along the edge of the mask, the mask is always on the left side, as shown in the following figure. I input the coordinates of point 1, 2, 3, 4, 5, 6 respectively.

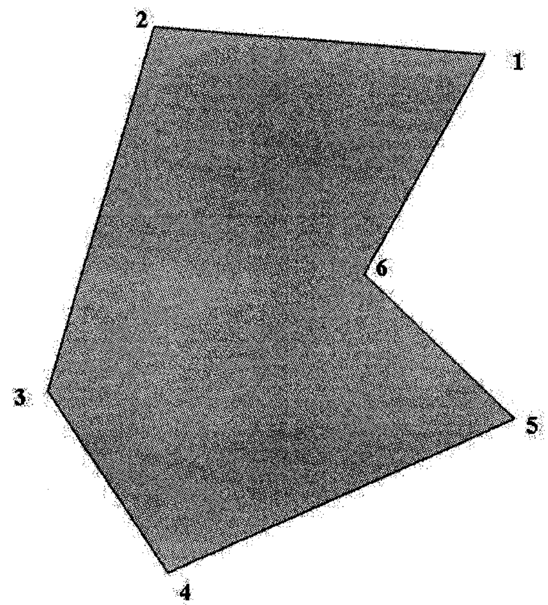

Figure 3–12: The input of mask coordinates in the computer

Whether it is a concave corner or convex corner is determined in the following way. Given a corner consisted of three points: 1, 2, 3, here point 2 is the apex of the corner, we can use two parameters to describe this corner: θ_1, θ_2, they are defined in the following diagram. And there are only four possibilities about the relation of θ_1 and θ_2, that is:

$$a : \theta_1 > \theta_2 and \theta_1 - \theta_2 < \pi \tag{3.14}$$

$$b : \theta_1 < \theta_2 and \theta_2 - \theta_1 < \pi \tag{3.15}$$

$$c : \theta_1 > \theta_2 and \theta_1 - \theta_2 > \pi \tag{3.16}$$

$$d : \theta_1 < \theta_2 and \theta_2 - \theta_1 > \pi \tag{3.17}$$

Fortunately, these four cases can be either a concave corner or a convex corner. e.g, case a and case d are convex corners, while case b and case c correspond to concave corners, as shown in the following figure.

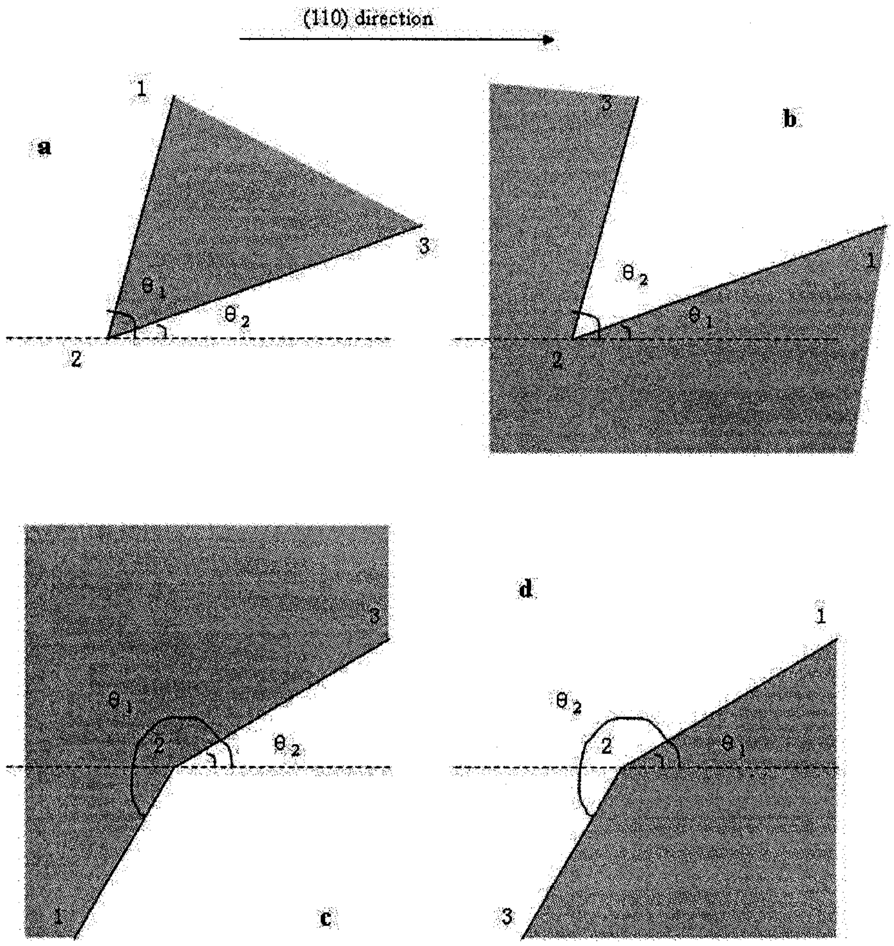

Figure 3–13: Distinguishing between the convex corner and concave corner. Case a: $\theta_1 > \theta_2 and \theta_1 - \theta_2 < \pi$ convex corner; Case b: $\theta_1 < \theta_2 and \theta_2 - \theta_1 < \pi$ concave corner; Case c: $\theta_1 > \theta_2 and \theta_1 - \theta_2 > \pi$ concave corner; Case d: $\theta_1 < \theta_2 and \theta_2 - \theta_1 > \pi$ convex corner;

Evolution of the corners in TMAH etching

In order to predict the etching result of TMAH, we need the ER diagram for TMAH etching. Below is the ER data I used, which is determined experimentally by the wagon wheel method in our lab.

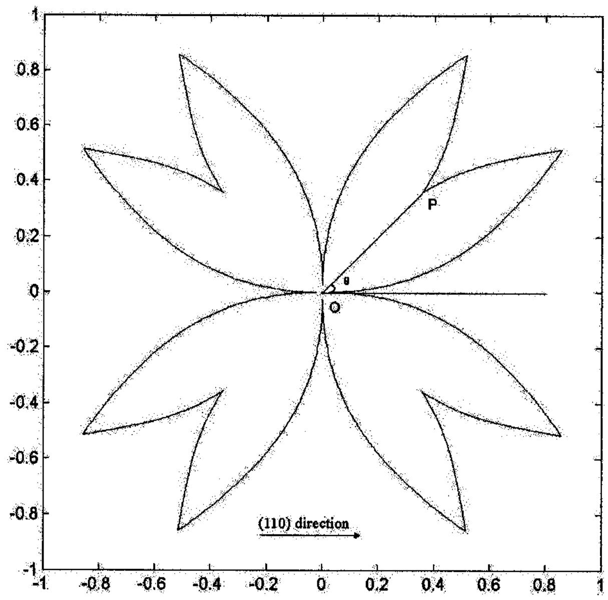

Figure 3–14: ER diagram of 25% TMAH at 85^oC. The unit of the axis is μm per minute. From this diagram we can find the ER of a given direction (θ) easily, for example, the distance of OP means the ER of (100)planes, whose intersect line with the wafer surface is along OP direction.

Convex Corner

In order to get the evolution of the corners in TMAH etching, we need to find the frontier of the etched structure, for example point P in the figure 3-15. Since for convex corners, the etched structure will be bounded by those fast etching planes, so the coordinates of point P can be determined using the following formula:

$$OP = maximum \frac{ER(\theta) * T}{sin(\theta - \alpha)} \tag{3.18}$$

Here we choose different θ and find the maximum. ER(θ) is the ER along θ direction and can be found from the ER diagram of TMAH, figure 3-14, α is the direction of OP, the range of θ in the loop of the program has been pointed out in the figure 3-15. The range is a little different in those four cases a, b, c, d.

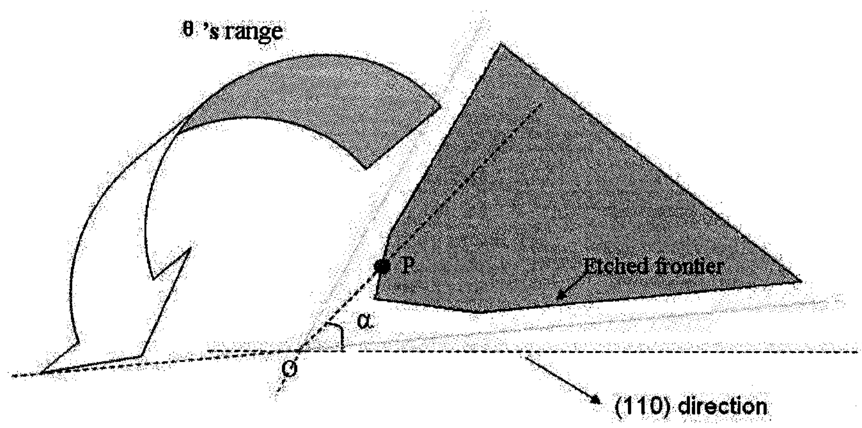

Figure 3–15: The frontier of the convex corner after TMAH etching. The yellow line is the original corner, the gray part is the etched shape, and α means the direction of OP. The arrow on the left side of the figure indicates the range of θ in the program code.The position of P can be determined by the distance OP and α.

Concave Corners

For concave corners, the situation is similar, just in formula 3.18, the maximum should be changed to minimum because now the etched shape is determined by the slow etching planes.

3.2.2 Simulation Results

The simulation results are quite the same as the experiment results.

Figure 3-16 is a square opening along the (100) direction after TMAH etching, the (111) planes come out in the concave corners.

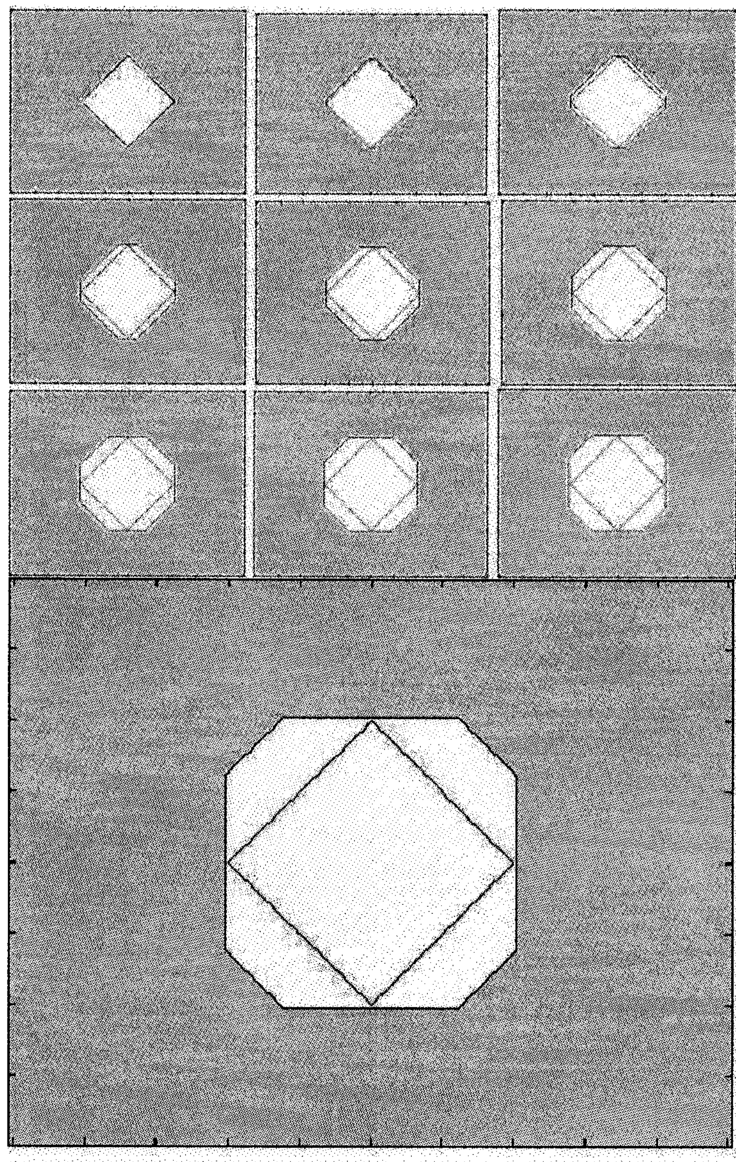

Figure 3–16: The simulation result of a square opening. The red line is the original shape of the opening, the blank area is the exposed silicon, and the unit of the axis is 150 μm. The square is along (100) direction, and the time step of the figures in the simulation is 30 minutes.

Figure 3-17 is an triangular opening, compared to the SEM view, we can see the simulation result agrees quite well with the experiment result.

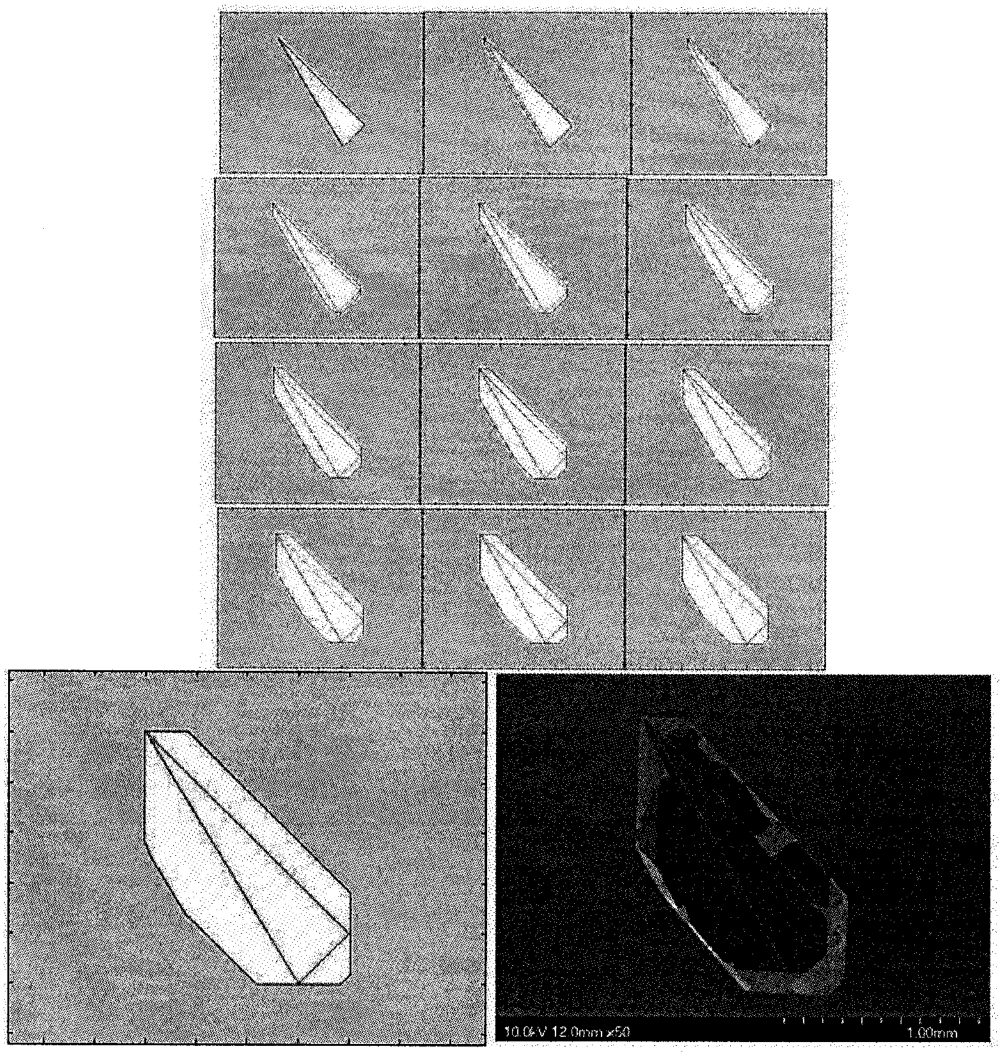

Figure 3–17: The simulation result of a triangular opening. The unit on the axis is 250 μm, and the time step of the simulation is 25 minutes. The image on the bottom-right corner is the experiment result of the same shape triangular opening after 6 hours TMAH etching.

Also, the simulator can be used to test the corner compensation design. Below are two examples. Figure 3-18 is using (110) strips as the corner compensation and figure 3-19 is using a small pad as the corner compensation:

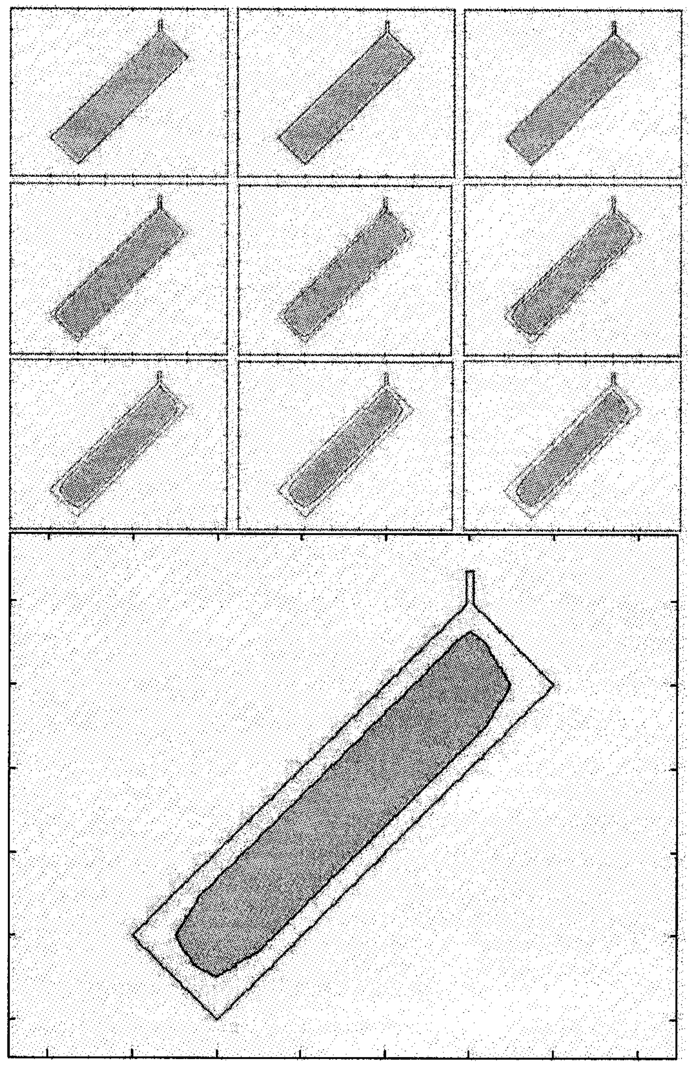

Figure 3–18: Simulation of (110) strips used as the corner compensation. Time step of the simulation is 3 minutes, and the unit on the axis is 100 μm.

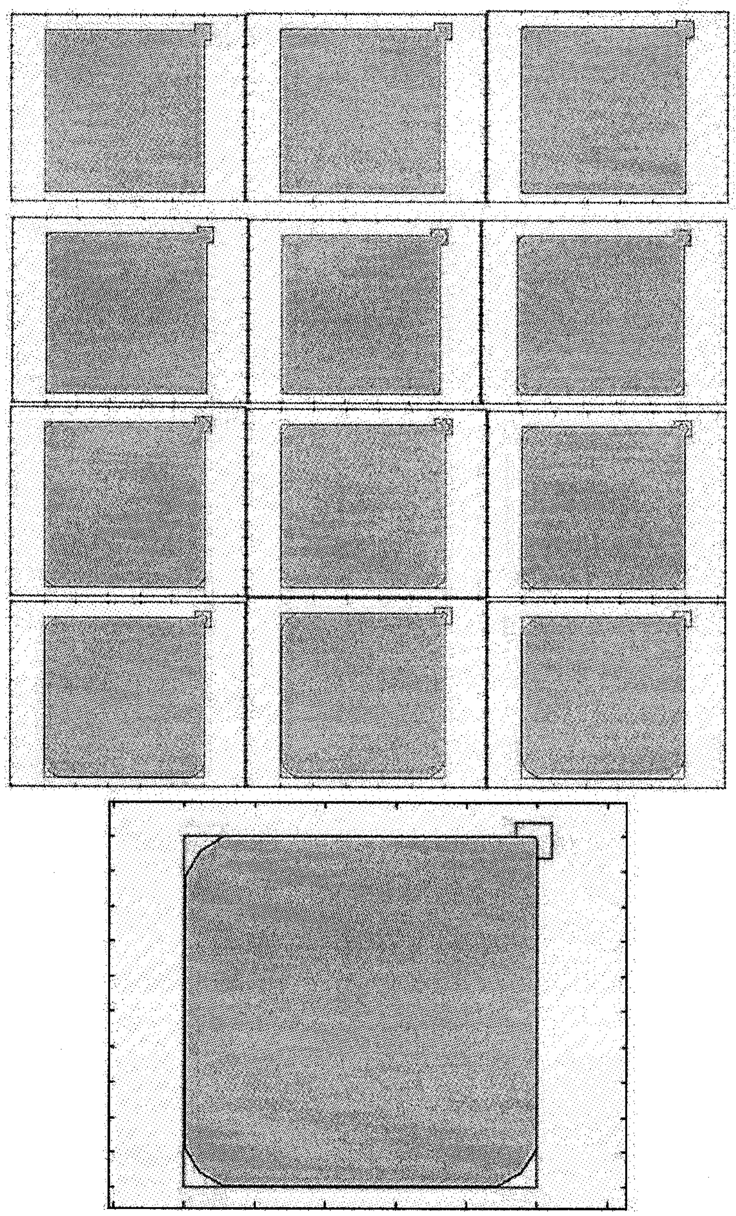

Figure 3–19: Simulation result of a small pad added on the corner for the corner compensation. The square is along the (110) direction. Time step of the simulation is 5 minutes, and the unit on the axis is 200 μm.

In both of these masks, I only included the corner compensation on one of the corners and we can see that the difference is very obvious. My program works very well in 2D view, and is helpful in designing the mask. To do the 3D simulation, it needs the 3D ER data of TMAH, which can be obtained from etching of a silicon sphere.

CHAPTER 4
Application

Bulk micromachining has many application in the integrated circuits industry and related industries such as microsystems/MEMS. For example, we can use the micromachining techniques to fabricate cantilevers which are used in AFM. Below is a scheme of the AFM and the right part is a typical cantilever with a tip on it.

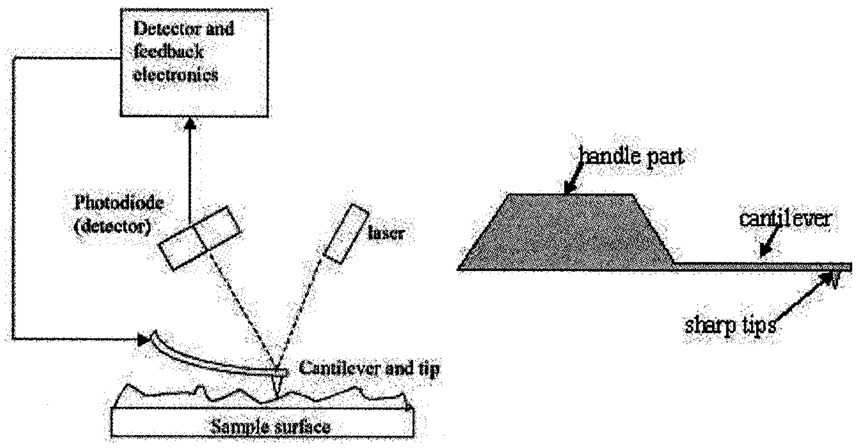

Figure 4–1: A simple diagram showing the principle of AFM

The following section will focus on making AFM cantilevers based on the knowledge of TMAH wet etching.

4.1 Silicon Oxide Cantilevers

The main material for the cantilevers is silicon, however, to make silicon cantilevers requires the SOI wafers, which are relatively expensive. Below is the process of making silicon cantilevers using SOI wafers [36].

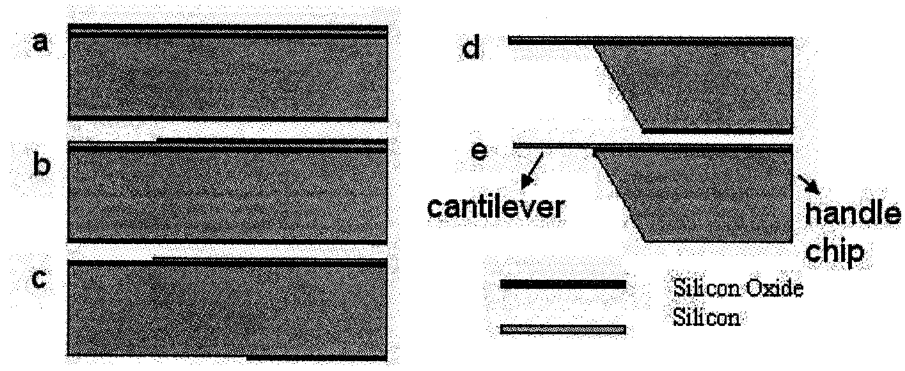

Figure 4–2: Process of making silicon cantilevers using SOI wafer. a: Oxidation. b: Pattern the topside oxide. c: Silicon etching and pattern the backside oxide. d: TMAH etching. e: remove the oxide film.

The process seems easy, but in fact it involves many issues. For example, how to do the alignment of the backside pattern to the frontside pattern? how to make the handle part so that it can be easily removed from the whole wafer? how to avoid the breaking of cantilevers when removing the handle from the wafer?

Before using expensive SOI wafers. I tested the basic processes by making oxide cantilevers, which are rather simple to make. The first step is to grow a thermal oxide film on top of the silicon wafer, in my experiment, the thickness is $1.5\mu m$. The second step is to transfer the pattern using RIE. Finally, the 3D structure is machined by TMAH wet etching.

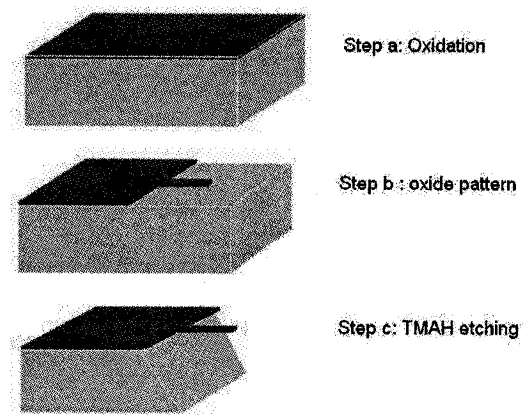

Figure 4–3: The process for making silicon oxide cantilevers.

Below is the results of the experiment.

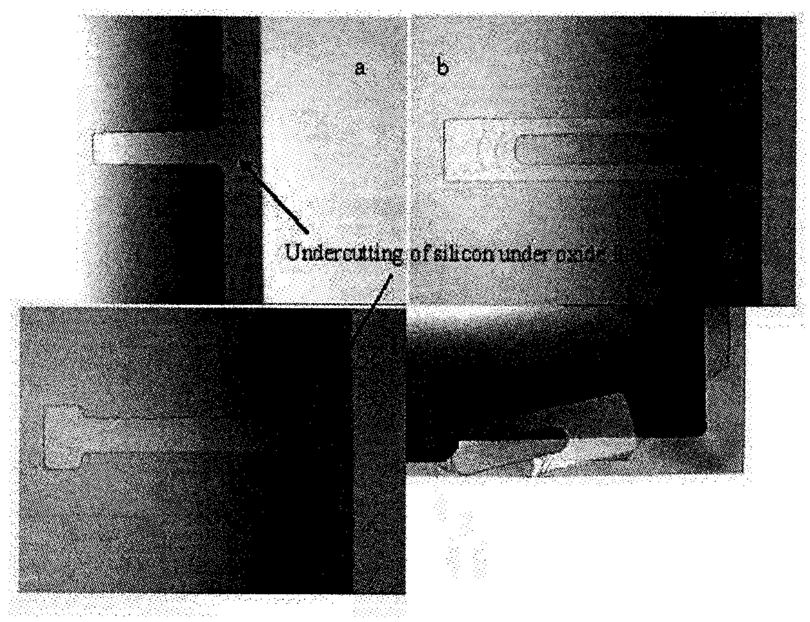

Figure 4–4: Optical images of oxide cantilevers. a: 160 μm long rectangular cantilever. b: 320 μm long cantilever. c: 300 μm long cantilever. d: A broken cantilever.

The shortcoming of oxide cantilevers is that the oxide film is very fragile so we need to be very careful when handling it. And there is an issue coming along with this process. That is the silicon below the oxide film will be undercut during the etching process. Though the edge of the mask is aligned to the (110) direction and the ER of (111) is very slow, the undercutting is about $70\mu m$ when we etch through the 6 inch wafer which is $675\mu m$ thick. We can notice this clearly from the following figure.

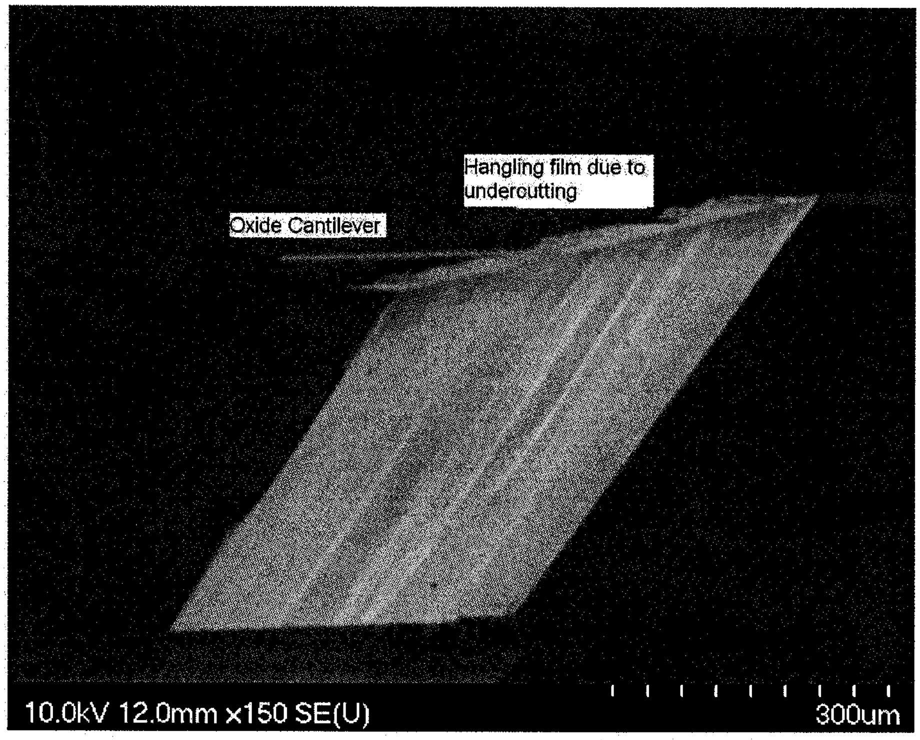

Figure 4–5: The oxide cantilevers and the undercutting.

Also, since the AFM use the optical method to detect the bending of the cantilevers, the cantilevers made from the above process is not suitable for normal AFM imaging. The reason is that the inclined sidewall will block the laser path, shown in the following figure. It can, however, be used for special applications such as cantilever based sensing.

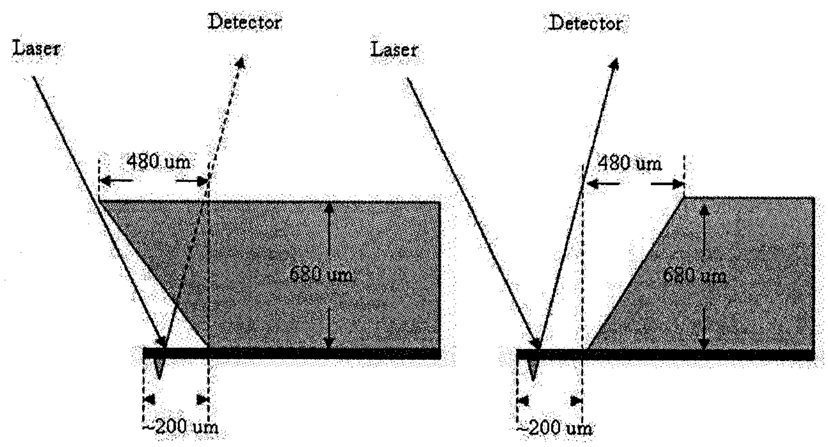

Figure 4–6: The AFM cantilever. Left: incorrect design. Right: correct design.

4.2 Silicon Nitride Cantilevers

In order to get rid of the undercutting and solve the light path blockade problem, we can use silicon nitride as the material for cantilevers, and use the following process.

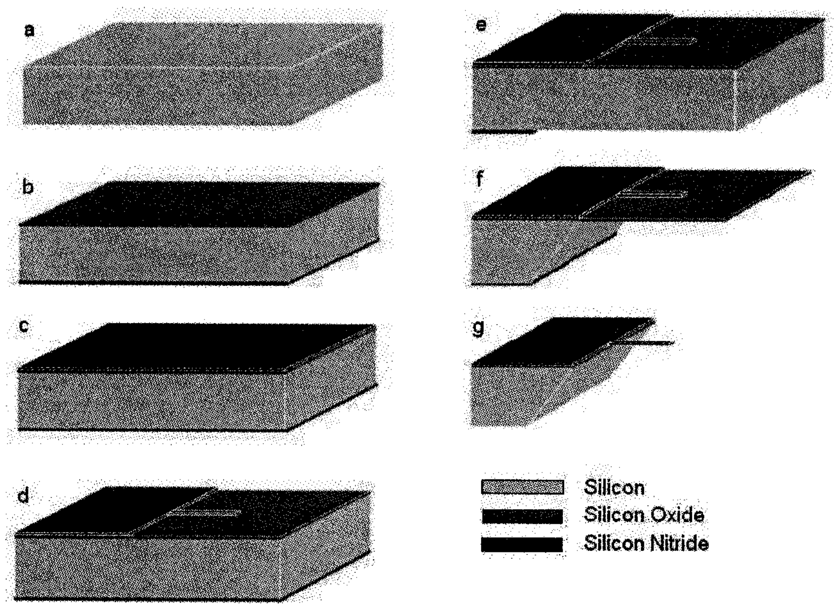

Figure 4–7: The process for fabricating silicon nitride cantilevers. a: starting material (100) wafer. b: Grow oxide on both side. c: Deposit silicon nitride on the top surface. d: Pattern the silicon nitride film. e: Pattern the backside oxide. f: TMAH etching. g: Release of nitride cantilever in HF.

In step c, a silicon nitride layer of thickness $1.0\mu m$ was deposited on the wafer using LPCVD method. In step e, we need to align the backside pattern to the top side pattern. The accuracy of the top-bottom alignment in our fab can be within 5 μm by a proper alignment mark design and carefully control of the alignment tool. In step g, most of the nitride film were broken along with the breaking of the large area oxide film. How to avoid this is still under development. Besides this, since the property, eg. the density, of the deposited silicon nitride film is not the same, the

ER of the nitride in RIE is very different. In our experiment, the ER of 0.5 μm/min, 0.2 μm/min, 0.1 μm/min were measured in the same recipe of RIE on three wafers with LPCVD nitride on. The reason is not clear yet.

4.3 Making the Handle part

The beam and the tip are the core of the AFM cantilever, however, the handle part is also very important because it is used as a holder for the AFM cantilever. The typical dimension of the handle part is $3,400\mu m$ by $1,600\mu m$. For the commercial available cantilevers, there are hundreds of chips included in one single wafer. So the requirement of the handle part is that it holds steady to the silicon frame, and at the same time can easily and safely be detached from the frame. Usually, the design looks like the following:

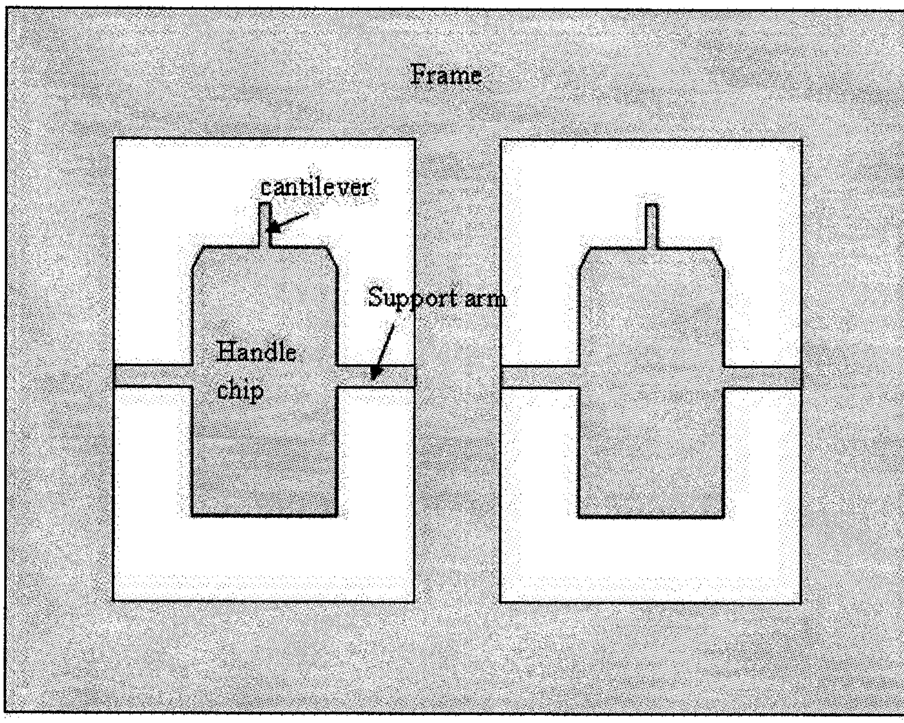

Figure 4–8: Cantilever chips with frame. The handle chip for a commercial AFM cantilever is 1,600 μm by 3,400 μm, The support arm should be strong enough to prevent the breaking by a small perturbation, but at the same time can easily and safely be detached from the frame using tweezers.

4.3.1 Supporting Arm

First of all, the strength of the supporting arm needs to be proper, strong enough to survive small vibration and weak enough so that it can be easily broken with tweezers. Since it is along the (110) direction, and the ER for the (111) plane is very slow, if in the mask, the width for the supporting arm is too large, then at the end of the etching, the thickness of the supporting arm is the same as the wafer, and this is so thick that it is very difficult to break the arms. And if the width for the supporting arm is too small, the arm will be totally etched after etching through the wafer. According to the experiment, the width of the supporting arm should be around 60 $\sim$ 80μm, as shown in figure 4-9.

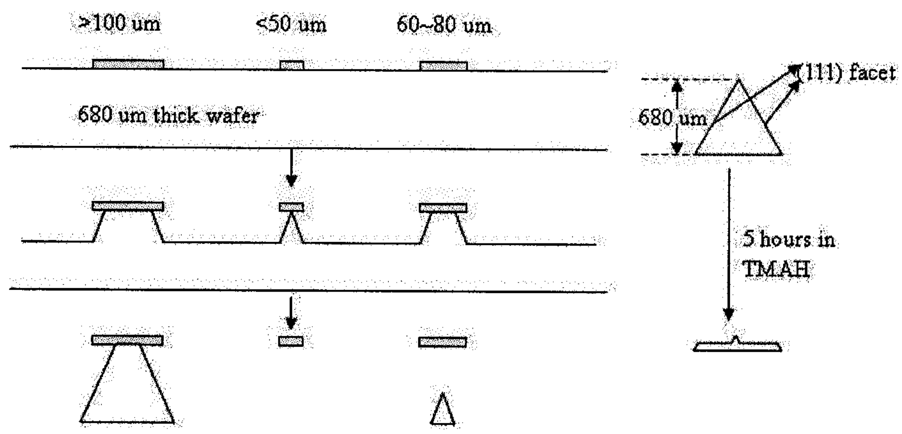

Figure 4–9: The width of the supporting arm. The mask should be carefully designed. If the width is too large(left), then the arm remaining after etching is too strong to break; if the width is too small(center), it will be totally removed.

However, when doing this, I found that sometimes, it worked well, but sometimes all the supporting arms disappeared. This is caused by the misalignment of the mask to the wafer flat. When the silicon wafer comes out from industry, the wafer flat is made along (110) direction, so we can align our mask to the wafer flat. However, the precision on the flat is about 3^o [6], and since the ER in the neighbor of (111) plane increases very fast with the departure from (111) plane, it may result in much faster undercutting due to the misalignment in the (110) direction. We can see it clearly from the following picture.

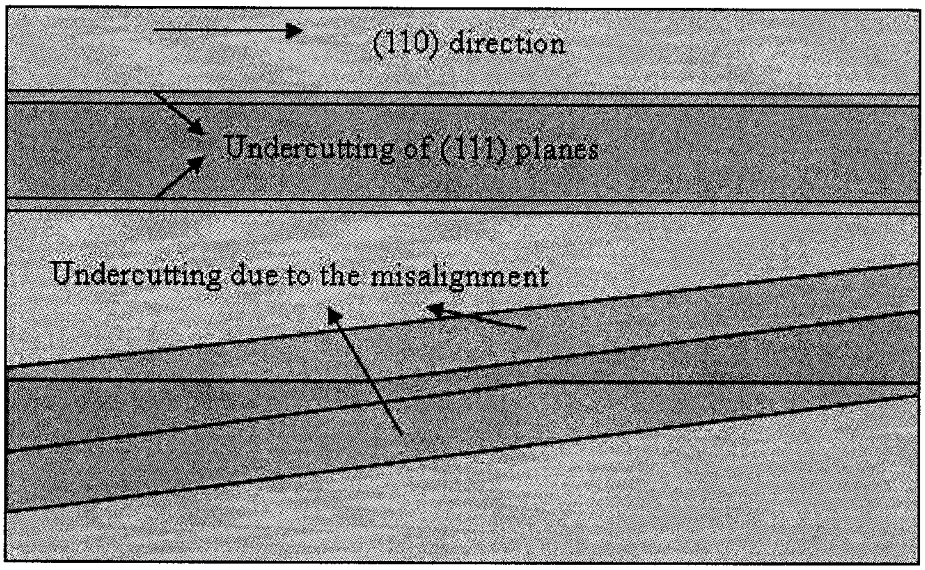

Figure 4–10: The misalignment of the mask may cause serious errors. The beam along the (110) direction will be quickly etched if it is not aligned very well to the (110) direction.

To solve the problem, we can use the property of the anisotropic etching, that is the slowest etched (111) plane. We can make a rectangular opening on the oxide film first, then put it in the TMAH for the pre-etching. After several hours etching, the etched pit will be formed by (111) planes. Because the oxide film is transparent, the (110) intersection line is visible under the alignment tool. So now we can use the (110) edge to do the alignment instead of using the wafer flat. This method is shown in the following figure.

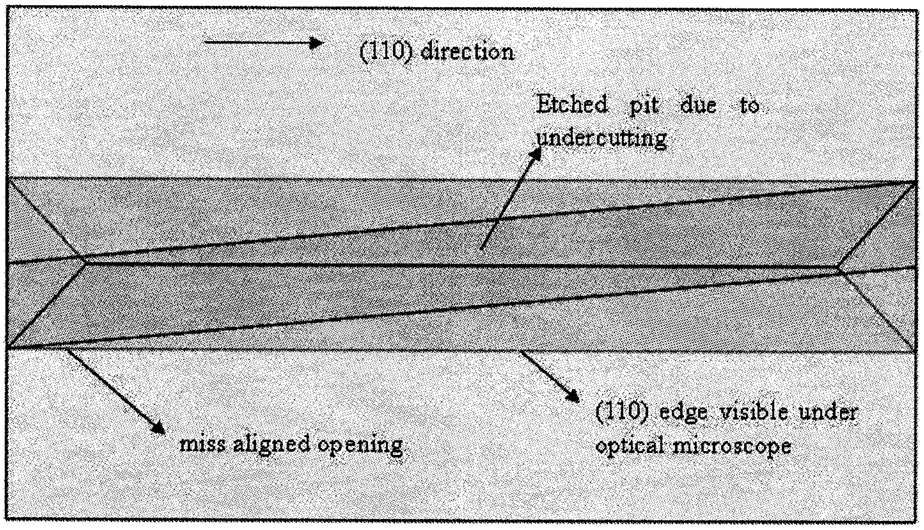

Figure 4–11: Method for align the mask to the (110) direction. The edge of the etched pit is along the (110) direction, and it is visible under the alignment tool, so it can be used to align the mask to the (110) direction instead of using the wafer flat.

Figure 4-12 is the optical images of two grooves. Rectangle a was aligned to the (110) direction using the method mentioned above while b was just aligned to the wafer flat. From the figure, we can see that in the bottom one, the oxide film opening was not parallel to the edge of the etched pit, which means it was not aligned to the (110) direction very well. Though it seems just a small difference, it may cause serious problems in the process, just like the disappearance of those supporting arms mentioned above.

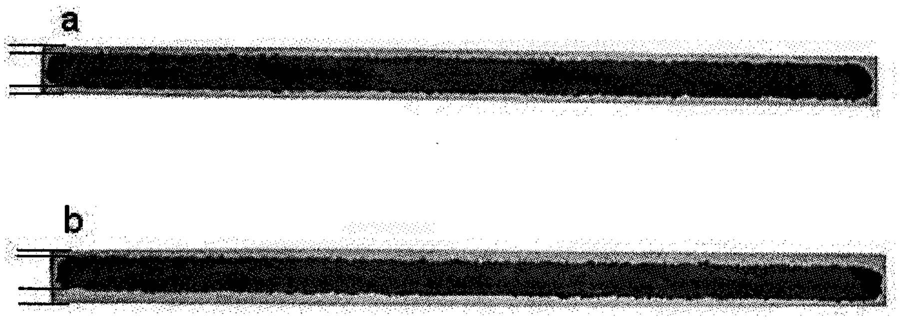

Figure 4–12: The etched pits of rectangular opening. The rough rectangle is the oxide mask opening with a width of 20 μm, and the underneath rectangle is the etched pit. The upper one was aligned to the (110) direction using the method mentioned above while the bottom one was just aligned to the wafer flat. Comparing the gap between those small lines, we can find that the bottom one was not aligned very well to the (110) direction.

After using this method as the alignment, the result of the supporting arm is reproducible. The width of the arm is about $800\mu m$, while the thickness is about $300\mu m$, and it is easy to break.

4.3.2 Corner Compensation for the Chip

Since we need to etch through the wafer, if we don't include any corner compensation in the mask design, the chip will be completely etched before the wafer is etched through. As said before, if we use (110) strips, the length of the strips is about $3,000\mu m$, which needs a lot of space. Actually, I used the folded strips to do the corner compensation shown in the following. The reason for connecting the strips to the outside mask is that it can further reduce the space for corner compensation.

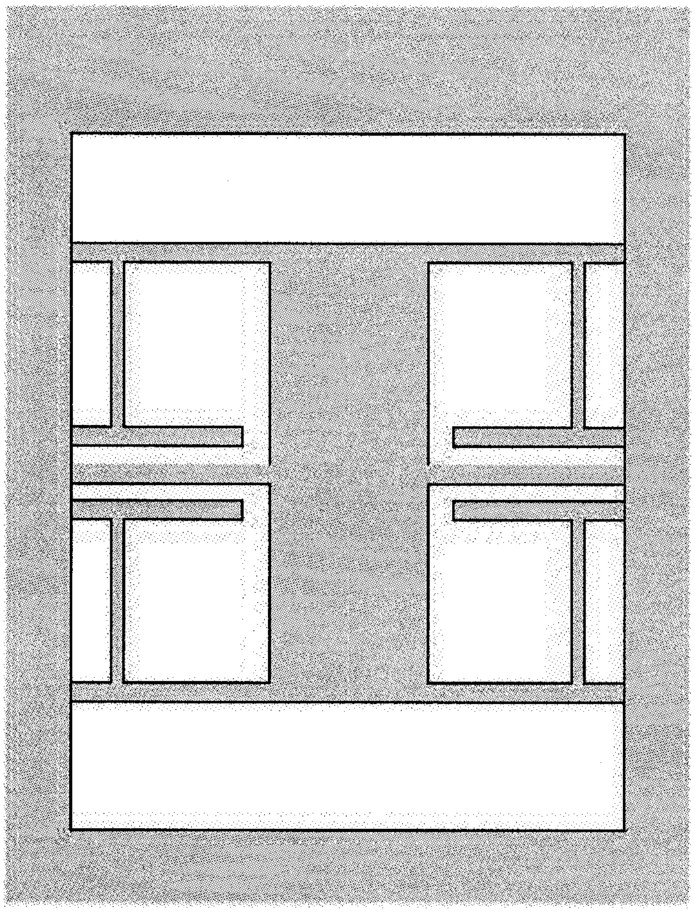

Figure 4–13: (110) strips with two turns were used to do the corner compensation.

I included difference length of strips in my mask, and the result is that, for short strips, although the chip survived, the corners was round off quite a lot, and for long strips, the residue caused by (411) sidewalls made the corner not a normal one.

The dimension of the chip is shown in the following figure.

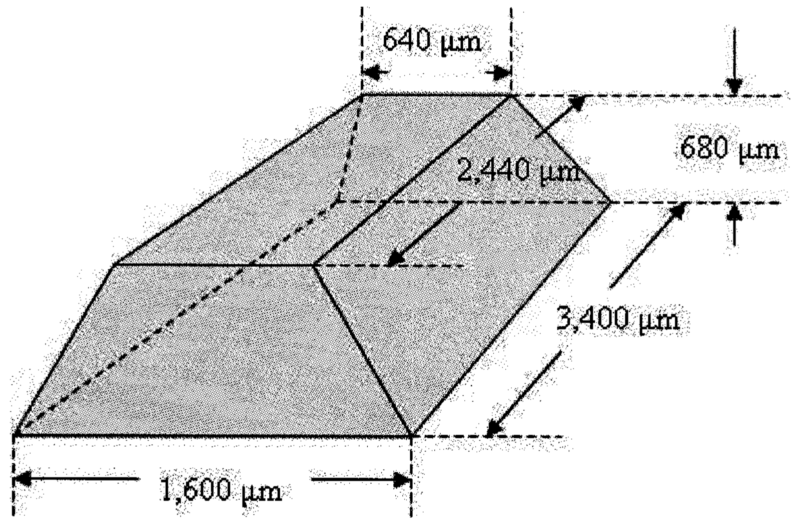

Figure 4–14: Dimension of the chip

If we use (100) strips as the corner compensation, the width for those strips should be twice the etching depth. For example, if the etching depth is the thickness of the wafer, the width is $2 * 680 = 1,360\mu m$, that is too wide to be included in the mask. However, we can first put the wafer in the TMAH solution to reduce the thickness, say, thin the wafer to $400\mu m$, then we can use the (100) strips in this situation.

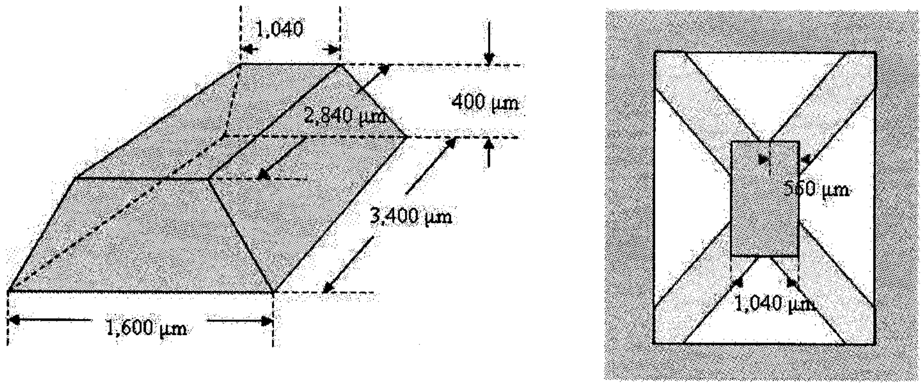

Figure 4–15: (100) strips for the corner compensation of thin wafer

The results are shown in the following figure. The left one is the result of using (110) strips as corner compensation, as we can see in the figure, the corner compensation is not enough. The right one is the result of using (100) strips. It looks very good.

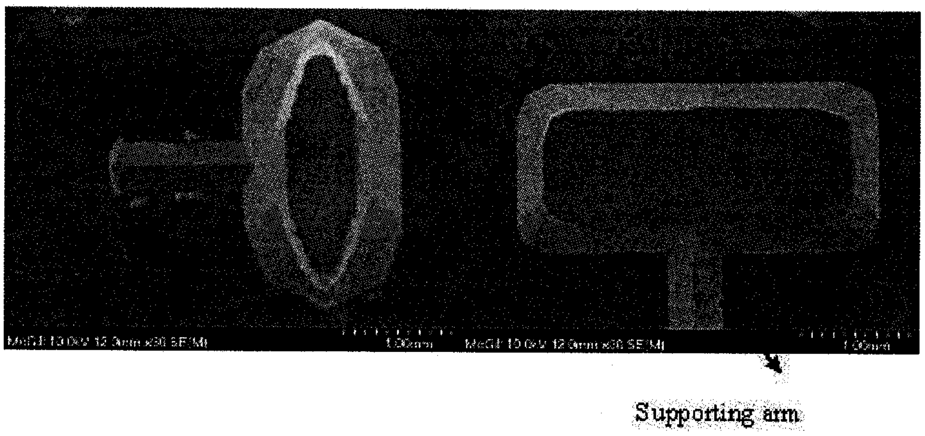

Figure 4–16: The handle chip of the cantilever. Left: using (110) strips in figure 4-13 as the corner compensation, the corners were still underetched very much. Right: using (100) strips as the corner compensation. Much better result came out.

4.4 Silicon Cantilevers

The most frequently used starting material for silicon cantilevers is a SOI wafer because of its simplicity and reproducibility. However, there are some other methods in making silicon cantilevers [37, 38], and these are all based on the time etch stop. One group reported making (100) oriented cantilevers using the following process [39]. I tried out this process, but found that it was indeed difficult to succeed in it. The timing is a big problem, so the etched depth is not predictable. What's more, since the PR is spun on the surface and the thickness of the PR is no more than $2\mu m$, the sidewalls of the etched structure couldn't be coated with PR in step c, so the experiment failed.

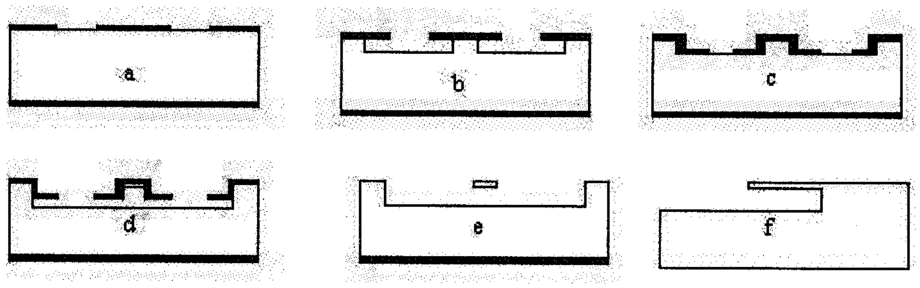

Figure 4–17: A method to make (100) oriented silicon cantilevers. a: Pattern the top oxide. b: TMAH etching. The etch depth should be controlled. c: Remove the oxide and reoxidation, then pattern the top oxide again. d: TMAH etching. e: Remove the oxide film. f: A side view of the fabricated cantilever.

4.4.1 Making Tips

Besides the cantilever, the tip is also a very important part of the AFM probe. The most efficient way to make a tip is using the undercutting of the anisotropic etchant to make a pyramid and then re-oxidize it for tip sharpening [18, 37, 40, 41].

The process is shown in figure 4-18. The first step is to grow oxide on the silicon wafer as the mask, then pattern the oxide mask, and then put it in TMAH solution for a certain time followed by re-oxidizing it. After the reoxidation, the tip will be sharpened. Finally, remove the oxide.

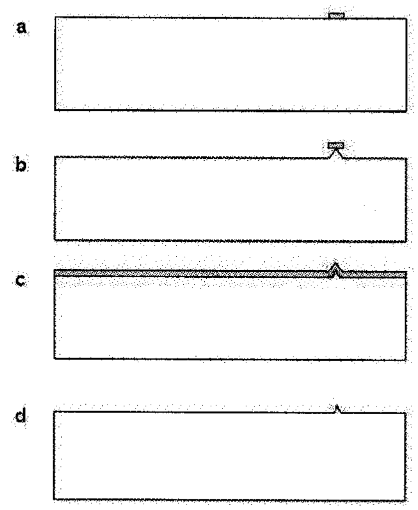

Figure 4–18: The anisotropic etching process for making tips. a: Pattern the top oxide. b: TMAH etching. c: Remove the oxide and reoxidize it. d: Remove the oxide.

Below is the pyramids after 40 minutes TMAH etching using square masks with size 60*60 μm. The facets of the pyramids are (411) planes.

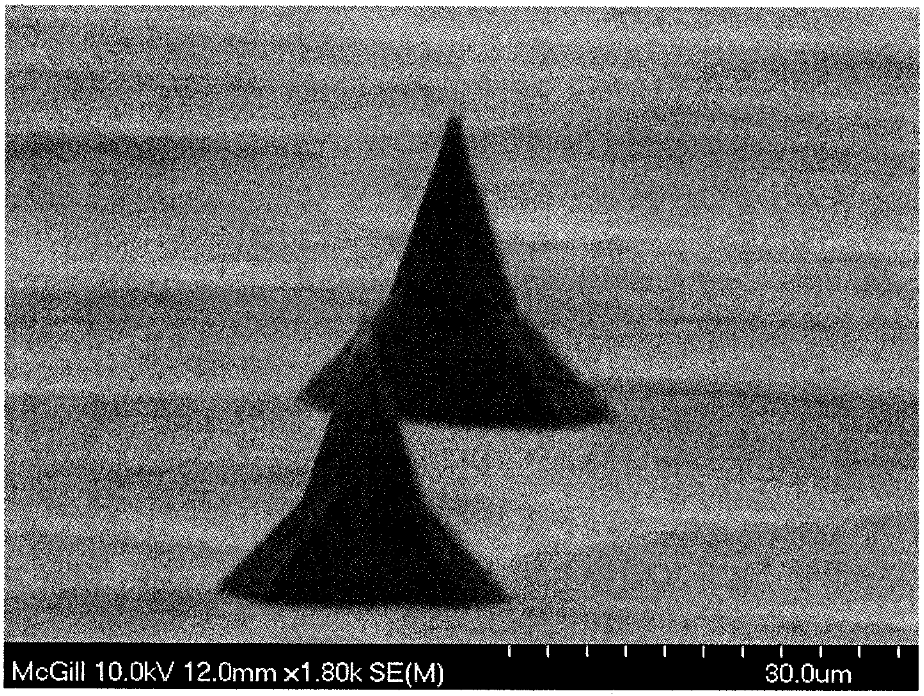

Figure 4–19: The pyramids made by anisotropic TMAH etching.

The size of the mask should be designed properly. If it is too small, the sharp tip will disappear, and if the mask is too large, then the tip is not formed yet, as shown in the following figure. The etching time is 40 minutes, the size of the mask is $65 * 65\mu m$, $60 * 60\mu m$, $55 * 55\mu m$ respectively (from top to bottom).

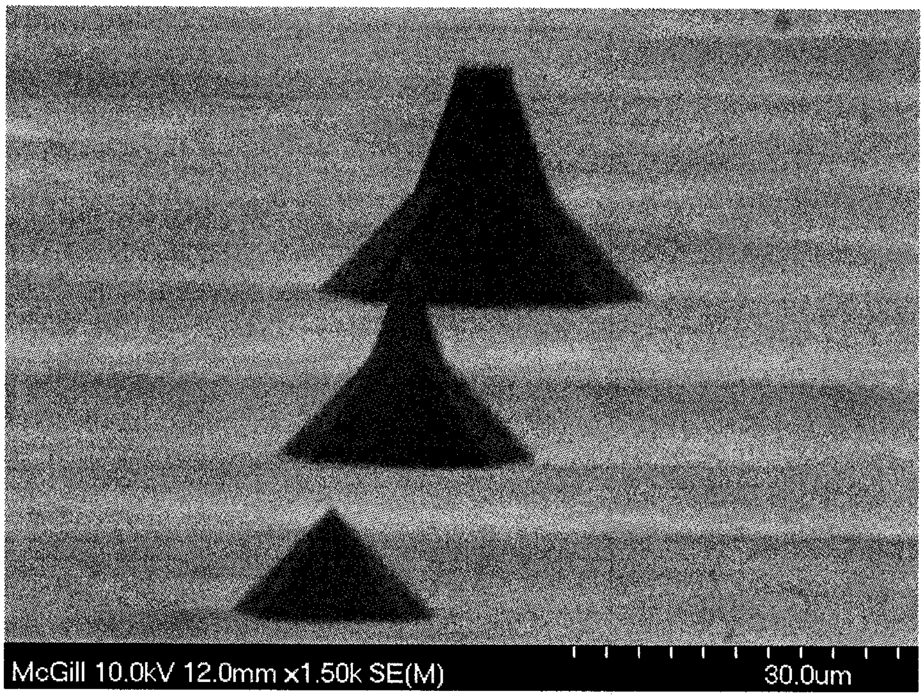

Figure 4–20: The results of different size of masks

In a AFM probe, a cantilever with integrated tip is used. The process is a combination of the above processes and it needs the alignment of those masks, see figure 1-1 and patent US6,006,265 by Galvin, US6,156,216 by Manalis, US5,066,358 by Quate and US5,399,232 by Albrecht for reference.

CHAPTER 5
Conclusions and outlook

After one year's research in wet bulk micromachining using TMAH, I have obtained some experience in microfabrication, including the etching properties of TMAH, the basic processes in lithography and the mask making. Also, some application of wet etching was performed.

The ER of TMAH is one of the problem we often encounter in the experiments. It is not well controlled, so we always use fresh solution to get repeatable results. And due to the limitation of the resolution of the mask used, the minimum size of the fabricated structure is around $10\mu m$, to get smaller feature, we need high resolution mask. Silicon oxide cantilevers were made using wet etching, but due to some stress problems, the result is not very good.

My future research will be continued on the application of TMAH etching. For example, to make silicon cantilever using SOI wafers. After that, the processes for more complicated structure will be tested, such as piezoresistive cantilevers [42] and capacitive cantilevers [43].

APPENDIX A
Mask Making

For my research, the masks are made in out fab. The process is first to design the mask in computer using AutoCAD. Secondly, send the mask file to a company, which can print it out on a transparency with high resolution. There are many companies in North America doing such things, such as www.pageworks.com(US), www.typoexpress.com(Canada). Then transfer the mask pattern to a quartz plate with a chrome film on one side using lithography. Finally, selectively etching the chrome. This mask can be used both in the stepper (reduction of feature sizes by a factor of 5) or in the EVG mask aligner. The scheme is shown below.

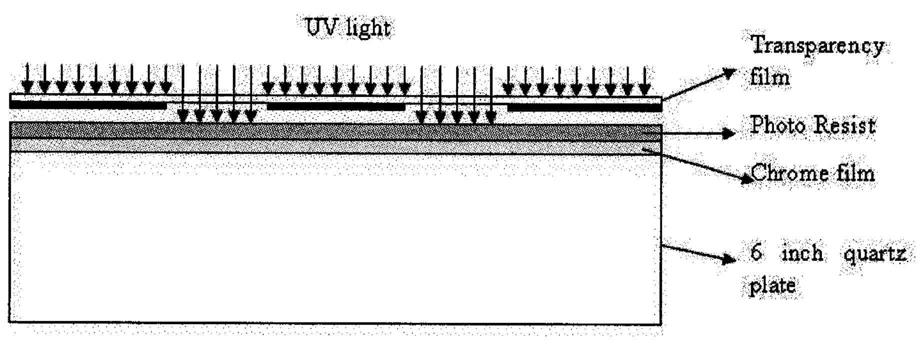

Figure A–1: The sketch process to make a mask

Actually, the transparency is in contact with the plate during the UV exposing. Since the pattern is printed out just on one side of the transparency, we should make sure that in the UV light exposing step, the side with the pattern on faces down.

Otherwise, due to the thickness of the transparency, the pattern will be deformed by the diffraction.

The advantage of making mask by ourselves is that, it is quick and cheap. Typoexpress is a local company which offers the printing of the transparency, so it only takes one day to get the transparency after the finish of mask design. And the price is $20 \sim 50$ dollars, depending on the resolution needed. The disadvantage is that the resolution is not very high. The critical size on the transparency is $20\mu m$, and the edge of the mask made by this method is rough. In our fab, we have a stepper, which can transfer the pattern on the mask to the wafer with a ratio of 5:1. So any dimension below $4\mu m$ is not acceptable in this method.

If high resolution masks are needed, they need to be made by a special company, and the price is often very high, above $1,000$ dollars. And usually it takes a week or so to make the mask and deliver it. So for the establish of the processes in our fab, we made the masks by ourself to save money and time.

APPENDIX B
Equipment in our fab

EVG Aligner The EVG aligner is very useful in lithography. It is used to make the mask, UV light exposing, and alignment. It can hold 6 inch wafer, and the resolution is $0.5\mu m$.

SpinBall Coater/Developer This equipment is used to deposit various type of PR on the substrate. Sample of size 1 square meter to 6 inch wafer is acceptable.

Furnaces There are four stack of furnace inside the cleanroom. One is for thermal oxidation, and it is in use currently, both wet and dry oxidation is available. The other ones are for doping, polysilicon deposition, silicon nitride deposition. These three furnaces are still under construction.

Applied P5000 4 Chamber RIE These four chambers are used for dry etching. Champer A is for oxide and nitride etching. Chamber B is for silicon and polysilicon etching. Chamber C is for metals etching. Chamber D is to be decided.

Surface Profilometer This tool is used for observing the topography of the sample. It is useful in measuring the etch depth after TMAH etching. The resolution can be $\dot{A}$.

Inspection Microscope It is used to view the sample. $X5, X10, X20, X50, X100$ amplification is available.

Tyger Reflectometer It is used to measure the thickness of a certain film on the substrate. The film can be PR, oxide, nitride, etc.

Silicon Wet Bench It is used for TMAH etching. It has temperature control, and rinsing tank aside.

HF Bench The diluted HF is used to remove the native oxide or release structure after the TMAH etching. As HF is quite a strong acid, it should be careful when handling it.

E-beam Evaporator This is used for metal deposition. Aluminum, silver, titanium targets are available.

Critical Point Dryer This tool is reserved to dry very tiny and fragile structures, such as cantilevers.

The above is the mostly used equipment for my research, and there are many other tools in our fab. For details, visit http://www.physics.mcgill.ca/nanotools/.

APPENDIX C
Simulation Code

The program is written in Matlab language.

```
--------------------------------------------

--    Main Program for the Simulation      --

--------------------------------------------


function [S,H]=Mask(X,T)

%X=[0,0;750,-1250;1000,-1000];T=200;

%X=[0,0;10,10;0,20;-10,10];T=40;

%X=[0,0;0,10;10,10;10,0];T=40;

%X=[0,0;0,100;20,100;20,0];T=40;

%X=[0,0;50,50;0,100;-50,50];T=100

Xmin=min(X(:,1))-T; Xmax=max(X(:,1))+T; Ymin=min(X(:,2))-T;

Ymax=max(X(:,2))+T; Initial_X=[X(:,1);X(1,1)];

Initial_Y=[X(:,2);X(1,2)]; [Sstart,Mstart]=GetCorner(X); S=Sstart;

KSstart=parrel(Sstart); H=moviein(T); for t=1:T

    TryS=S+Mstart;

    KTryS=parrel(TryS);

    Judge=KTryS.*KSstart;

    Condition=sum(Judge');
```

```
if all(Condition>0)
    S=TryS;
else
    Cond=(Condition>0);
    L_Cond=length(Cond);
    GoodPoint=find(Cond);
    BadPoint=find(1-Cond);
    %L_Good=length(GoodPoint);
    %GoodPointplus=[GoodPoint(L_Good),GoodPoint];
    %NewSstart=[];
    %NewMstart=[];
    X1=S(BadPoint(1),1);
    X2=S(BadPoint(1)+1,1);
    Y1=S(BadPoint(1),2);
    Y2=S(BadPoint(1)+1,2);
    time1=(X2-X1)/(Mstart(BadPoint(1),1)-Mstart(BadPoint(1)+1,1));
    time2=(Y2-Y1)/(Mstart(BadPoint(1),2)-Mstart(BadPoint(1)+1,2));
    time=min(time1,time2);
    Newcorner=S(GoodPoint,:)+time*Mstart(GoodPoint,:);
    [Sstart,Mstart]=GetCorner(Newcorner);
    S=Sstart+Mstart*(1-time);
    KSstart=parrel(Sstart);
end
```

```
    plot(Initial_X,Initial_Y,'r',S(:,1),S(:,2),'b');
    axis([Xmin Xmax Ymin Ymax]);axis square;axis equal;
    %hold on;
    %plot(S(:,1),S(:,2),'b*');
    %hold off;
    H(:,t)=getframe;
end



%-------------------------------------------
function [S,M]=GetCorner(V) N=size(V); N=N(1); S=[]; M=[];
Y=[V(N,:);V;V(1,:)]; for k=2:N+1
    G=Y(k-1:k+1,:);
    P=Anglerevolution(G);
    Qx=G(2,1)+0.01*P(:,1);
    Qy=G(2,2)+0.01*P(:,2);
    Q=[Qx Qy];
    S=[S;Q];
    M=[M;P];
end S=[S;S(1,:)]; M=[M;M(1,:)];

%---------------------
```

```
%function Angle_S=Angle(S)
%N=length(S);
%for p=1:N-1
    %Angle_S(p)=Period(S(p,1),S(p,2),S(p+1,1),S(p+1,2));
    %end
%Angle_S=[Angle_S,Angle_S(1)];

%-----------------------
function KS=parrel(S)
L=length(S); KS=S(2:L,:)-S(1:L-1,:);


%---------------------
function R=Crosspoint(P1,P2,P3,P4)
a=(P4(1)-P3(1))*(P1(2)-P3(2))-(P4(2)-P3(2))*(P1(1)-P3(1));
b=(P4(2)-P3(2))*(P2(1)-P1(1))-(P4(1)-P3(1))*(P2(2)-P1(2)); t=a/b;
R(1)=P1(1)+t*(P2(1)-P1(1)); R(2)=P1(2)+t*(P2(2)-P1(2));

-------------------------------
--    Several sub-program     --
-------------------------------
```

The program Anglerevolution is to judge whether it is a concave corner or a convex corner and find the etched result of a single corner.

Program Anglerevolution

```
%-------------------------------------------
function P=Anglerevolution(G)
%G is a 3 by 2 matrix. T is the etching time.
%G=[0,10;0,0;-10,0];
X1=G(1,1);Y1=G(1,2); X2=G(2,1);Y2=G(2,2); X3=G(3,1);Y3=G(3,2);
Delta=0.005; theta1=Period(X2,Y2,X3,Y3);
theta2=Period(X2,Y2,X1,Y1);
%---------case 1
if (theta2>theta1)&&(theta2-theta1<pi)
    %it is a concave corner
    delta=Delta;
    alpha_vector=theta2+delta:delta:2*pi+theta1-delta;
    theta_vector=theta2:delta:pi+theta1;
    [alpha,theta]=meshgrid(alpha_vector,theta_vector);
    L=length(alpha_vector);
    ThetaMatrix=theta_vector'*ones(1,L);
    Denominator=sin(alpha-theta).*(sin(alpha-theta)>0)+..
    1e-30*delta*(sin(alpha-theta)<=0);
    Denominator=abs(Denominator);
```

```
t=Etchrate(ThetaMatrix)./Denominator;
[Y,I]=min(t);
a=0;b=theta_vector(I(1));
for p=1:L
    if (abs(theta_vector(I(p))-b)>0.1)
        a=a+1;
        angle_alpha(a)=alpha_vector(p);
        angle_theta(a)=theta_vector(I(p));
        D(a)=Y(p);
        b=theta_vector(I(p));
    end
end
Alpha=angle_alpha;
Theta=angle_theta;
Theta_1=Theta+0.1;
while (any(abs(Theta-Theta_1)>1e-20))
    for pp=1:a
        theta_vector=Theta(pp)-delta:0.1*delta:Theta(pp)+delta;
        Denominator=sin(Alpha(pp)-theta_vector).*(sin(Alpha(pp)-theta_v..
        ector)>0)+1e-30*delta*(sin(Alpha(pp)-theta_vector)<=0);
        Denominator=abs(Denominator);
        t=Etchrate(theta_vector)./Denominator;
        [Y,Index]=min(t);
```

```
        D(pp)=Y;
        angle_theta(pp)=theta_vector(Index);
    end
    Theta_1=Theta;
    Theta=angle_theta;
    delta=delta*0.1;
end
for s=1:a
    P3=[X2+D(s)*cos(Alpha(s)),Y2+D(s)*sin(Alpha(s))];
    P4=P3+[cos(Theta(s)),sin(Theta(s))];
    if s==1
        P1=[X2+Etchrate(theta2)/sin(0.01)*cos(theta2+0.01),Y2+..
        Etchrate(theta2)/sin(0.01)*sin(theta2+0.01)];
        P2=P1+[cos(theta2),sin(theta2)];
    else
        P1=[X2+D(s-1)*cos(Alpha(s-1)),Y2+D(s-1)*sin(Alpha(s-1))];
        P2=P1+[cos(Theta(s-1)),sin(Theta(s-1))];
    end
    if s==a
        P3=[X2+Etchrate(theta1)/sin(0.01)*cos(theta1-0.01),Y2+..
        Etchrate(theta1)/sin(0.01)*sin(theta1-0.01)];
        P4=P3+[cos(theta1),sin(theta1)];
    end
```

```
        R(s,:)=Crosspoint(P1,P2,P3,P4);
    end
%--------------------case2
elseif (theta2>theta1)&&(theta2-theta1>pi)
    %it is a convex corner
    delta=Delta;
    alpha_vector=theta2+delta:delta:2*pi+theta1-delta;
    theta_vector=theta1:delta:theta2-pi;
    [alpha,theta]=meshgrid(alpha_vector,theta_vector);
    L=length(alpha_vector);
    ThetaMatrix=theta_vector'*ones(1,L);
    Denominator=sin(alpha-theta);
    Denominator=abs(Denominator);
    t=Etchrate(ThetaMatrix)./Denominator;
    [Y,I]=max(t);
    a=0;b=theta_vector(I(1));
    for p=1:L
        if (abs(theta_vector(I(p))-b)>0.1)
            a=a+1;
            angle_alpha(a)=alpha_vector(p);
            angle_theta(a)=theta_vector(I(p));
            D(a)=Y(p);
            b=theta_vector(I(p));
```

```
    end
end
Alpha=angle_alpha;
Theta=angle_theta;
Theta_1=Theta+0.1;
while (any(abs(Theta-Theta_1)>1e-20))
    for pp=1:a
        theta_vector=Theta(pp)-delta:0.1*delta:Theta(pp)+delta;
        Denominator=sin(Alpha(pp)-theta_vector);
        Denominator=abs(Denominator);
        t=Etchrate(theta_vector)./Denominator;
        [Y,Index]=min(t);
        D(pp)=Y;
        angle_theta(pp)=theta_vector(Index);
    end
    Theta_1=Theta;
    Theta=angle_theta;
    delta=delta*0.1;
end
for s=1:a
    P3=[X2+D(s)*cos(Alpha(s)),Y2+D(s)*sin(Alpha(s))];
    P4=P3+[cos(Theta(s)),sin(Theta(s))];
    if s==1
```

```
            P1=[X2+Etchrate(theta2)/sin(0.01)*cos(theta2+0.01),Y2+..
            Etchrate(theta2)/sin(0.01)*sin(theta2+0.01)];
            P2=P1+[cos(theta2),sin(theta2)];
        else
            P1=[X2+D(s-1)*cos(Alpha(s-1)),Y2+D(s-1)*sin(Alpha(s-1))];
            P2=P1+[cos(Theta(s-1)),sin(Theta(s-1))];
        end
        if s==a
            P3=[X2+Etchrate(theta1)/sin(0.01)*cos(theta1-0.01),Y2+..
            Etchrate(theta1)/sin(0.01)*sin(theta1-0.01)];
            P4=P3+[cos(theta1),sin(theta1)];
        end
        R(s,:)=Crosspoint(P1,P2,P3,P4);
    end
%------------------case 3
elseif (theta2<theta1)&&(theta1-theta2<pi)
    %it is a convex corner
    delta=Delta;
    alpha_vector=theta2+delta:delta:theta1-delta;
    theta_vector=theta1:delta:theta2+pi;
    [alpha,theta]=meshgrid(alpha_vector,theta_vector);
    L=length(alpha_vector);
    ThetaMatrix=theta_vector'*ones(1,L);
```

```
Denominator=sin(alpha-theta);
Denominator=abs(Denominator);
t=Etchrate(ThetaMatrix)./Denominator;
[Y,I]=max(t);
a=0;b=theta_vector(I(1));
for p=1:L
    if (abs(theta_vector(I(p))-b)>0.1)
        a=a+1;
        angle_alpha(a)=alpha_vector(p);
        angle_theta(a)=theta_vector(I(p));
        D(a)=Y(p);
        b=theta_vector(I(p));
    end
end
Alpha=angle_alpha;
Theta=angle_theta;
Theta_1=Theta+0.1;
while (any(abs(Theta-Theta_1)>1e-20))
    for pp=1:a
        theta_vector=Theta(pp)-delta:0.1*delta:Theta(pp)+delta;
        Denominator=sin(Alpha(pp)-theta_vector);
        Denominator=abs(Denominator);
        t=Etchrate(theta_vector)./Denominator;
```

```
        [Y,Index]=min(t);
        D(pp)=Y;
        angle_theta(pp)=theta_vector(Index);
    end
    Theta_1=Theta;
    Theta=angle_theta;
    delta=delta*0.1;
end
for s=1:a
    P3=[X2+D(s)*cos(Alpha(s)),Y2+D(s)*sin(Alpha(s))];
    P4=P3+[cos(Theta(s)),sin(Theta(s))];
    if s==1
        P1=[X2+Etchrate(theta2)/sin(0.01)*cos(theta2+0.01),Y2+..
        Etchrate(theta2)/sin(0.01)*sin(theta2+0.01)];
        P2=P1+[cos(theta2),sin(theta2)];
    else
        P1=[X2+D(s-1)*cos(Alpha(s-1)),Y2+D(s-1)*sin(Alpha(s-1))];
        P2=P1+[cos(Theta(s-1)),sin(Theta(s-1))];
    end
    if s==a
        P3=[X2+Etchrate(theta1)/sin(0.01)*cos(theta1-0.01),Y2+..
        Etchrate(theta1)/sin(0.01)*sin(theta1-0.01)];
        P4=P3+[cos(theta1),sin(theta1)];
```

```
        end
        R(s,:)=Crosspoint(P1,P2,P3,P4);
    end
%-----------------------case4
else
    %it is a concave corner
    delta=Delta;
    alpha_vector=theta2+delta:delta:theta1-delta;
    theta_vector=theta2:delta:theta1-pi;
    [alpha,theta]=meshgrid(alpha_vector,theta_vector);
    L=length(alpha_vector);
    ThetaMatrix=theta_vector'*ones(1,L);
    Denominator=sin(alpha-theta).*(sin(alpha-theta)>0)+..
    1e-30*delta*(sin(alpha-theta)<=0);
    Denominator=abs(Denominator);
    t=Etchrate(ThetaMatrix)./Denominator;
    [Y,I]=min(t);
    a=0;b=theta_vector(I(1));
    for p=1:L
        if (abs(theta_vector(I(p))-b)>0.1)
            a=a+1;
            angle_alpha(a)=alpha_vector(p);
            angle_theta(a)=theta_vector(I(p));
```

```
        D(a)=Y(p);
        b=theta_vector(I(p));
    end
end
Alpha=angle_alpha;
Theta=angle_theta;
Theta_1=Theta+0.1;
while (any(abs(Theta-Theta_1)>1e-20))
    for pp=1:a
        theta_vector=Theta(pp)-delta:0.1*delta:Theta(pp)+delta;
        Denominator=sin(Alpha(pp)-theta_vector).*(sin(Alpha(pp)-..
        theta_vector)>0)+1e-30*delta*(sin(Alpha(pp)-theta_vector)<=0);
        Denominator=abs(Denominator);
        t=Etchrate(theta_vector)./Denominator;
        [Y,Index]=min(t);
        D(pp)=Y;
        angle_theta(pp)=theta_vector(Index);
    end
    Theta_1=Theta;
    Theta=angle_theta;
    delta=delta*0.1;
end
for s=1:a
```

```
        P3=[X2+D(s)*cos(Alpha(s)),Y2+D(s)*sin(Alpha(s))];
        P4=P3+[cos(Theta(s)),sin(Theta(s))];
        if s==1
            P1=[X2+Etchrate(theta2)/sin(0.01)*cos(theta2+0.01),Y2+..
            Etchrate(theta2)/sin(0.01)*sin(theta2+0.01)];
            P2=P1+[cos(theta2),sin(theta2)];
        else
            P1=[X2+D(s-1)*cos(Alpha(s-1)),Y2+D(s-1)*sin(Alpha(s-1))];
            P2=P1+[cos(Theta(s-1)),sin(Theta(s-1))];
        end
        if s==a
            P3=[X2+Etchrate(theta1)/sin(0.01)*cos(theta1-0.01),Y2+..
            Etchrate(theta1)/sin(0.01)*sin(theta1-0.01)];
            P4=P3+[cos(theta1),sin(theta1)];
        end
        R(s,:)=Crosspoint(P1,P2,P3,P4);
    end
end

%Q=length(D);
%Alpha(1)=theta2+asin(Etchrate(theta2)/D(1));
%Alpha(Q)=theta1-asin(Etchrate(theta1)/D(Q));
```

```
Unitx=R(:,1)-X2; Unity=R(:,2)-Y2; P=[Unitx,Unity];
%plot([X1,X2,X3],[Y1,Y2,Y3],'b-');
%hold on;
%plot(R(:,1),R(:,2),'ro');



%-------------------------------------------------------
function R=Crosspoint(P1,P2,P3,P4)
a=(P4(1)-P3(1))*(P1(2)-P3(2))-(P4(2)-P3(2))*(P1(1)-P3(1));
b=(P4(2)-P3(2))*(P2(1)-P1(1))-(P4(1)-P3(1))*(P2(2)-P1(2)); t=a/b;
R(1)=P1(1)+t*(P2(1)-P1(1)); R(2)=P1(2)+t*(P2(2)-P1(2));

function theta=Period(Xb,Yb,Xe,Ye) if (Xe-Xb)~=0
    beta=atan((Ye-Yb)/(Xe-Xb));
    C1=(Ye>=Yb)&(Xe>=Xb);
    C23=(Xe<Xb);
    C4=(Ye<Yb)&(Xe>=Xb);
    theta=beta*C1+(2*pi+beta)*C4+(pi+beta)*C23;
elseif Ye>Yb
    theta=pi/2;
else
    theta=1.5*pi;
```

```
end
%--------------------------------
function ER=Etchrate(theta)
%theta=pi/4;
global ER100 ER111 ER411 a=-1; b=-1; theta0=pi/4-atan(0.25);
beta1=0.5*theta0; beta2=0.5*(theta0+pi/4);
theta=theta-0.5*pi*floor(2*theta/pi);
J1=(theta>=0)&(theta<=theta0); J2=(theta>theta0)&(theta<=pi/4);
J3=(theta>pi/4)&(theta<=pi/2-theta0); J4=(theta>pi/2-theta0);
F1=(ER411+ER111)/2+(ER411-ER111)/2*tan(2*(2-exp(-a))*..
   (theta-beta1)/(4*theta0/pi))/tan((2-exp(-a))*pi/4);
F2=(ER411+ER100)/2+(ER411-ER100)/2*tan(2*(2-exp(-b))*..
   (theta-beta2)/(4*theta0/pi-1))/tan((2-exp(-b))*pi/4);
F3=(ER411+ER100)/2+(ER411-ER100)/2*tan(2*(2-exp(-b))*..
   (pi/2-theta-beta2)/(4*theta0/pi-1))/tan((2-exp(-b))*pi/4);
F4=(ER411+ER111)/2+(ER411-ER111)/2*tan(2*(2-exp(-a))*..
   (pi/2-theta-beta1)/(4*theta0/pi))/tan((2-exp(-a))*pi/4);
ER=F1.*J1+F2.*J2+F3.*J3+F4.*J4;
```

References

[1] D.M. Eigler and E.K. Schweizer. *Nature*, 344:524–526, 1990.

[2] T.W. Fisklock, A. Oral, R.G. Egdell, and J.B. Pethica. *Nature*, 743:404, 2000.

[3] U.A. Dauderstadt, P.H.S. De Vries, R. Hiratsuka, and P.M. Sarro. *Sensors and Actuators A*, 46(1-3):201–204, Jan-Feb 1995.

[4] L.Richard Carley, Leon Abelmann, and Seungook Min. *Journal of Applied Physics*, 87(9), May 2000.

[5] Albert Folch, Mark S.Wrighton, and Martin A.Schmidt. *Journal of Microelectromechanical Systems*, 6(4), December 1997.

[6] Marc Madou. *Fundamentals of MICROFABRICATION*. CRC press, 1997.

[7] H. Seidel, L.Csepregi, A. Heuberger, and H. Baumgartel. *Journal of Electrochem. Soc.*, 137(11):3612–3626, November 1990.

[8] H. Jansen, M.de Boer, R. Legtenberg, and M. Elwenspoek. *Journal of Micromech. and Microeng.*, 5(2):115–120, June 1995.

[9] Kirt R. Williams and Richard S. Muller. *Journal of Microelectromechanical Systems*, 5(4), December 1996.

[10] Gregory T. A. Kovacs, Nadim I. Maluf, and Kurt E. Petersen. *Proceesings of the IEEE*, 86(8):1536–1551, August 1998.

[11] Jiunn jye Tsaur, Chen-Hsun Du, and Chengkuo Lee. *Sensors and Actuators A*, 92:375–383, 2001.

[12] J. Chen, L.T. Liu, Z.J. Li, Z.M. Tan, Q.S. Jiang, H.J. Fang, Y. Xu, and Y.X. Liu. *Sensors and Actuators A*, 96:15–156, 2002.

[13] Z. Elalamy, L.M. Landsberger, A. Pandy, M. Kahrizi, I. Stateikina, and S. Michel. *J. Vac. Sci. Technol. A*, 20(6):1927–1933, Nov/Dec 2002.

[14] I. Stateikina, Z. Elalamy, L.M. Landsberger, and M. Kahrizi. *J. Vac. Sci. Technol. A*, 22(3):1073–1077, May/Jun 2004.

[15] A. Pandy, L.M. Landsberger, B. Nikpour, M. Paranjape, and M. Kahrizi. *J. Vac. Sci. Technol. A*, 16(2):868–872, Mar/Apr 1998.

[16] K. Sato, M. Shikida, T. Yamashiro, K. Asaumi, Y. Iriye, and M. Yamamoto. *Sensors and Actuators A*, 73:131–137, 1999.

[17] X.P. Wu and W.H. Ko. *Sensors and Actuators A*, 18:207–215, 1989.

[18] H.L. Offereins, K. Kuhl, and H. Sandmaier. *Sensors and Actuators A*, 25-27:9–13, 1991.

[19] M Elwenspoek. *Journal of Electrochem. Soc.*, 140(7):2075–2080, 1993.

[20] T. Nunn and J. Angell. *Workshop on Indwelling Pressure Transducers and Systems*, pages 133–136, 1975.

[21] Elin Steinsland, Martin Nese, Anders Hanneborg, Ralph W. Bernstein, Halle Sandmo, and Gjermund Kittilsland. *Sensors and Actuators A*, 54:728–732, 1996.

[22] A. Merlos, M. Acero, M.H. Bao, J. Bausells, and J. Esteve. *Sensors and Actuators A*, 37-38:737–743, 1993.

[23] B.E. Deal and A.S. Grove. *J.Appl. Phys.*, 36:3770–3778, December 1965.

[24] P.M. Sarro, C.R. deBoer, E.Korkmaz, and J.M.W.Laros. *Sensors and Actuators A*, 67:175–180, 1998.

[25] A.F.Flannery, N.J.Mourlas, C.W.Storment, S.Tsai, S.H.Tan, J.Heck, D.Monk, and T.Kim. *Sensors and Actuators A*, 70:48–55, 1998.

[26] B. Puers and W. Sansn. *Sensors and Actuators A*, 21-23:1036–1041, 1990.

[27] M.Bao, C. Burrer, J. Esteve, J. Bausells, and S. Marco. *Sensors and Actuators A*, 37-38:727–732, 1993.

[28] H.L.Offereins, G.K. Mayer, H.Sandmaier, and K.Kuhl. *J. Electrochem. Soc.*, 137(12):3947–3950, 1990.

[29] B. Nikpour, L.M. Landsberger, T.J. Hubbard, M.Kahrizi, and A. Iftimie. *Sensors and Actuators A*, 66:299–307, 1998.

[30] *http://www.intellisensesoftware.com/.*

[31] *http://www.coventor.com/memulator/index.html.*

[32] O. Than and S. Buttgenbach. *Sensors and Actuators A*, 45:85–89, 1994.

[33] R.A. Buser and N.F. de Rooij. *Sensors and Actuators A*, 28:71–78, 1991.

[34] J.S. Danel and G. Delapierre. *Sensors and Actuators A*, 31:267–274, 1992.

[35] C.H. Sequin. *Sensors and Actuators A*, 34:225–241, 1992.

[36] Yanjun Tang, Ji Fang, Xiaodong Yan, and Hai feng Ji. *Sensors and Actuators B*, 97:109–113, 2004.

[37] J. Brugger, R.A. Buser, and N.F. de Rooij. *Sensors and Actuators A*, 34:193–200, 1992.

[38] O. Wolter, Th. Bayer, and J. Greschner. *J. Vac. Sci. Technol. B*, 9(2):1353–1357, May-Apr 1991.

[39] Wai shing Choi and Jan G. Smits. *Journal of Microelectromechanical Systems*, 2(2):82–86, June 1993.

[40] P.A. Rasmussen, J. Thaysen, S. Bouwstra, and A. Boisen. *Sensors and Actuators A*, 92:96–101, 2001.

[41] D. Saya, K. Fukushima, H. Toshiyoshi, G. Hashiguchi, H. Fujita, and H. Kawakatsu. *Sensors and Actuators A*, 95:281–287, 2002.

[42] G. Villanueva, J. Montserrat, F. Perez-Murano, G. Rius, and J. Bausells. *Jounal of Microelectronic Engineering*, 73, 2004.

[43] N. Blanc, J. Brugger, N.F. de Rooij, and U. Durig. *J. Vac. Sci. Technil. B*, 14(2):901–905, May/Apr 1996.

KEY TO ABBREVIATIONS